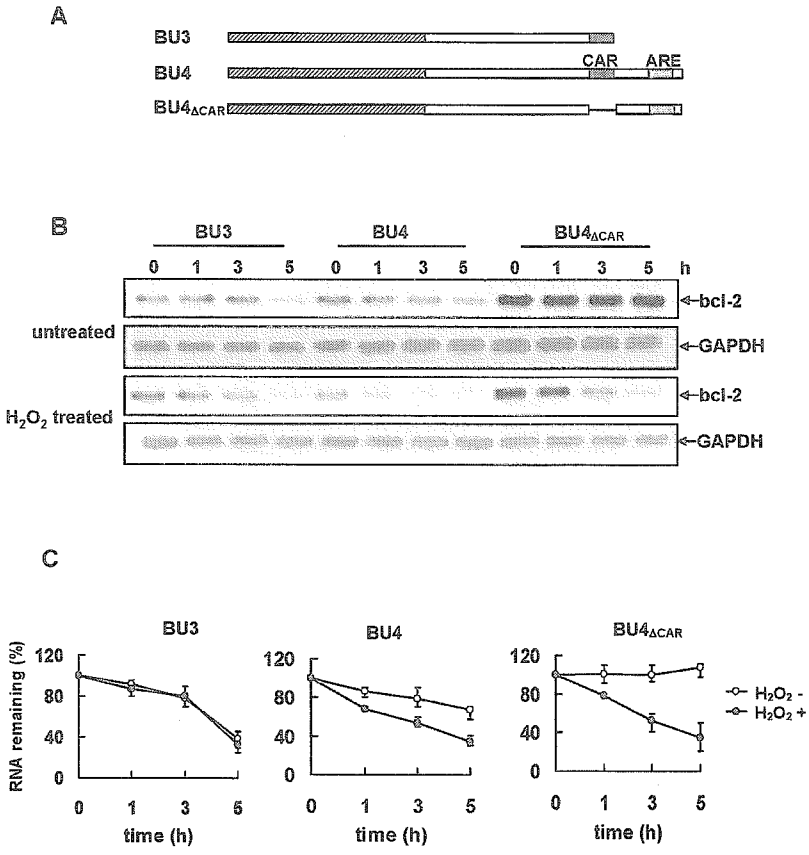

FIG. 5. **CA repeat-dependent decay of *bcl-2* mRNA is not enhanced by apoptosis.** COS7 cells were transiently transfected with three *bcl-2* constructs including CAR (BU3), ARE only ($BU4\Delta_{CAR}$), or both (BU4) in the 3′-UTR as shown in *A*, and *bcl-2* mRNA stability was analyzed in the presence of Act D. To induce apoptosis, H_2O_2 (1 mM) was added to cells 1 h prior to adding Act D (10 μg/ml). Total RNA was extracted at 0, 1, 3, or 5 h after Act D treatment and analyzed by Northern blot for *bcl-2* and subsequently for GAPDH as shown in *B*. *C*, *bcl-2* mRNA signals derived from the three constructs (BU3, BU4, and $BU4\Delta_{CAR}$) under normal and apoptotic condition were normalized with GAPDH mRNA signal from each lane in *B* after being quantified by densitometry using Scion image software (Scion Corp.). All data are represented as means ± S.D. from three independent experiments. *bcl-2* mRNA signal without Act D was defined as 100% and Act D-treated *bcl-2* mRNA levels were calculated as percentages of decay at the indicated times.

A

```
mouse_M16506.1_   533   TGAGGTCGACAAACCTGCCCCAAACAAATATGCAAAAGGTTCACTAAAGCAGTAGAAATTA-T
Rat_L14680_       942   TGAGGTCAGCAGACCTGCCCCAAACAAATATG-AAAAGGTTCACTAAAGCAGTAGAAATTAAT
Human_M13994_    2175   TGAAGTCAACATGCCTGCCCCAAACAAATATGCAAAAGGTTCACTAAAGCAGTAGAAATAA-T

mouse_M16506_          ATGCATTATCAATGATGTACCATGAAACAAAGTTGT-GATCTTTTTTTAAAGCAGAACACACA
Rat_L14680_            ATGCATTATCAAGGATGGACCATGAAACAAAGTTGT-GATTTTTTTTTAAAGCAGAACACACA
Human_M13994_          ATGCATTGTCAGTGATGTACCATGAAACAAAGCTGCAGGCTGTTTAAGAAAAAATAACACACA

mouse_M16506_          CACACACACACACACACACACACACACACACACACACACACA-------          697
Rat_L14680_            CACACACACACACACACACACACACACACACACACACACACACACA            1012
Human_M13994_          TATAAACAT-CACACACACAGACAGACACACACACACACAA-------           2339
```

B

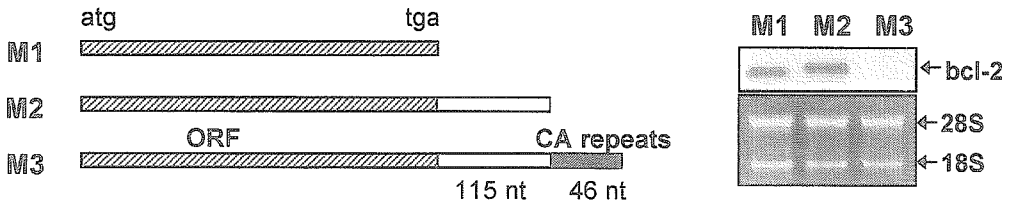

FIG. 6. **The nucleotide sequences and destabilization potential of an upstream portion of the 3′-UTR and CA repeats of the *bcl-2* gene are conserved in mammals.** *A*, the nucleotide sequences of the region upstream of the CA repeats in the 3′-UTR of *bcl-2* gene were compared for human, rat, and mouse (GenBank™ accession numbers on the *left*). Alignment was performed starting from the first nucleotide of the stop codon up to the last nucleotide of the CA repeats. The shared nucleotides among these three species are in *bold* and *underlined*. Multiple alignment comparison was performed using the ClustalW engine (www.justbio.com/aligner/). *B*, three constructs of mouse *bcl-2*, prepared as shown in the *left panel*, were transfected into COS7 cells, and *bcl-2* mRNA levels were analyzed (*right panel*).

rate of the *bcl-2* mRNA from the construct including the CA repeats but not the ARE was not significantly changed upon apoptosis induction, whereas *bcl-2* mRNA from the construct including the ARE and CA repeats was degraded faster under the same conditions (Fig. 5). Moreover, the transcript from the *bcl-2* DNA including the ARE but devoid of the CA repeats showed increased stability in nonapoptotic conditions but accelerated degradation in apoptotic conditions. Therefore, CA repeat-mediated decay of *bcl-2* appears to contribute to maintaining appropriate Bcl-2 levels in the steady states, while the ARE-dependent destabilizing pathway may react to apoptotic stimuli to permit a rapid down-regulation of the Bcl-2 level,

thereby leading to cell death. However, more diverse apoptotic stimuli should be applied to confirm the relevance of these two cis-elements in Bcl-2 down-regulation in apoptosis. Interestingly, the presence of Bcl-2 protein was previously proposed as an essential requirement for the activation of ARE-dependent degradation programs (19). We also found that the destabilizing effect induced by the incorporation of the upstream sequences and CA repeats of the 3′-UTR of *bcl-2* on GFP mRNA was less prominent than that of *bcl-2* mRNA (Fig. 3), raising the possibility that CA repeat-mediated decay also entails the presence of Bcl-2 protein. However, the coexpression of Bcl-2 did not influence the level of GFP mRNA with or without the 3′-UTR of the *bcl-2* gene in our study (data not shown). The amount of Bcl-2 protein was therefore not likely to be a critical prerequisite for the CA repeat-mediated decay of *bcl-2* mRNA, but another cis-element in the coding region of *bcl-2* might participate in the maintenance of the steady-state level of *bcl-2* mRNA. Another difference is that the presence of CA repeats in the 3′-UTR of *bcl-2* is confined to mammals, including humans, rats, and mice, whereas ARE is widely preserved, even being present in the 3′-UTR of nematode *bcl-2* (15). Moreover, the sequences 5′-upstream of the CA repeats also reveal a high level of homology in mammalian *bcl-2* (Fig. 6). Thus, CA repeat-mediated decay systems might have developed during evolutionary division into mammals to tune the *bcl-2* level more finely. The presence of diverse modes of regulating the Bcl-2 level, as shown in our report and in previous reports (15–17), suggests that different mechanisms are involved in the modulation of the Bcl-2 level in response to different physiological and pathological conditions.

Most of the mechanisms that regulate mRNA stability involve specific interactions between structural determinants on mRNA, cis-acting elements and proteins that bind the determinants, trans-acting proteins, which modulate the susceptibility of mRNA to degradation (32). Cis-acting elements could be an actual target site for ribonuclease, or they might regulate ribonuclease attack elsewhere in the mRNA by binding with either stabilizing or destabilizing factors. It has been shown previously that CA repeats or CA-rich sequences have the potential to bind proteins such as heterogeneous nuclear ribonucleoprotein (hnRNP) in the intron of eNOS pre-mRNA or in the 3′-UTR of vascular endothelial growth factor (VEGF) mRNA (28, 33). Therefore, defining whether a protein binds to the upstream sequences or CA repeats in the 3′-UTR of *bcl-2* and subsequently affects the *bcl-2* mRNA stability will be a subject of further investigation to get a complete understanding of the process of destabilizing *bcl-2* mRNA.

In conclusion, we describe a novel pathway of constitutive decay of *bcl-2* mRNA that involves CA repeats and their upstream sequences in the 3′-UTR, extending the functional significance of CA repeats from an intronic to an exonic context. Further investigation on the molecular mechanisms by which the CA repeats exert their destabilizing activity, including RNA/protein interactions, may contribute to the development of new strategies for reducing Bcl-2 levels in pathological conditions.

REFERENCES

1. Steller, H. (1995) *Science* **267,** 1445–1449
2. Tsujimoto, Y., Yunis, J., Onorato-Showe, L., Erikson, J., Nowell, P. C., and Croce, C. M. (1984) *Science* **224,** 1403–1406
3. Tsujimoto, Y., and Shimizu, S. (2000) *FEBS Lett.* **466,** 6–10
4. Bettaieb, A., Dubrez-Daloz, L., Launay, S., Plenchette, S., Rebe, C., Cathelin, S., and Solary, E. (2003) *Curr. Med. Chem. Anti-Canc. Agents* **3,** 307–318
5. Young, R. L., and Korsmeyer, S. J. (1993) *Mol. Cell. Biol.* **13,** 3686–3697
6. Miyashita, T., Harigai, M., Hanada, M., and Reed, J. C. (1994) *Cancer Res.* **54,** 3131–3135
7. Mayo, M. W., Wang, C-Y., Drouin, S. S., Madrid, L. V., Marshall, A. F., Reed, J. C., Weissman, B. E., and Baldwin, A. S. (1999) *EMBO J.* **18,** 3990–4003
8. Pugazhenthi, S., Miller, E., Sable, C., Young, P., Heidenreich, K. A., Boxer, L. M., and Reusch, J. E.-B. (1999) *J. Biol. Chem.* **274,** 27529–27535
9. Heckman, C. A., Mehew, J. W., Ying, G-G., Introna, M., Golay, J., and Boxer, L. M. (2000) *J. Biol. Chem.* **275,** 6499–6508
10. Perillo, B., Sasso, A., Abbondanza, C., and Palumbo, G. (2000) *Mol. Cell. Biol.* **20,** 2890–2901
11. Dimmeler, S., Breitschopf, K., Haendeler, J., and Zeiher, A. M. (1999) *J. Exp. Med.* **189,** 1815–1822
12. Breitschopf, K., Haendeler, J., Malchow, P., Zeiher, A. M., and Dimmeler, S. (2000) *Mol. Cell. Biol.* **20,** 1886–1896
13. Cheng, E. H., Kirsch, D. G., Clem, R. J., Ravi, R., Kastan, M. B., Bedi, A., Ueno, K., and Hardwick, J. M. (1997) *Science* **278,** 1966–1968
14. Del Bello, B., Valentini, M. A., Zunino, F., Comporti, M., and Maellaro, E. (2000) *Oncogene* **20,** 4591–4595
15. Schiavone, N., Rosini, P., Quattrone, A., Donnini, M., Lapucci, A., Citti, L., Bevilacqua, A., Nicolin, A., and Capaccioli, S. (2000) *FASEB J.* **14,** 174–184
16. Donnini, M., Lapucci, A., Papucci, L., Witort, E., Tempestini, A., Brewer, G., Bevilacqua, A., Nicolin, A., Capaccioli, S., and Schiavone, N. (2001) *Biochem. Biophys. Res. Commun.* **287,** 1063–1069
17. Lapucci, A., Donnini, M., Papucci, L., Witort, E., Tempestini, A., Bevilacqua, A., Nicolin, A., Brewer, G., Schiavone, N., and Capaccioli, S. (2002) *J. Biol. Chem.* **277,** 16139–16146
18. Luzi, E., Papucci, L., Schiavone, N., Donnini, M., Lapucci, A., Tempestini, A., Witort, E., Nicolin, A., and Capaccioli, S. (2003) *Cancer Gene Ther.* **10,** 201–208
19. Bevilacqua, A., Ceriani, M. C., Canti, G., Asnaghi, L., Gherzi, R., Brewer, G., Papucci, L., Schiavone, N., Capaccioli, S., and Nicolin, A. (2003) *J. Biol. Chem.* **278,** 23451–23459
20. Lee, J.-H., Takahashi, T., Yasuhara, N., Inazawa, J., Kamada, S., and Tsujimoto, Y. (1999) *Oncogene* **18,** 6183–6190
21. Thomson, A. M., Rogers, J. T., Walker, C. E., Staton, J. M., and Leedman, P. J. (1999) *BioTechniques* **27,** 1032–1042
22. Lander, E. S., Linton, L. M., Birren, B., Nusbaum, C., Zody, M. C., Baldwin, J., Devon, K., Dewar, K., Doyle, M., FitzHugh, W., Funke, R., Gage, D., Harris, K., Heaford, A., Howland, J., and *et al.* (2001) *Nature* **409,** 860–921
23. Gyapay, G., Morissette, J., Vignal, A., Dib, C., Fizames, C., Millasseau, P., Marc, S., Bernardi, G., Lathrop, M., and Weissenbach, J. (1994) *J. Nat. Genet.* **7,** 246–339
24. Dib, C., Faure, S., Fizames, C., Samson, D., Drouot, N., Vignal, A., Millasseau, P., Marc, S., Hazan, J., Seboun, E., Lathrop, M., Gyapay, G., Morissette, J., and Weissenbach, J. (1996) *Nature* **380,** 152–154
25. Pravica, V., Asderakis, A., Perrey, C., Hajeer, A., Sinnott, P. J., and Hutchinson, I. V. (1999) *Eur. J. Immunogenet.* **26,** 1–3
26. Agarwal, A. K., Giacchetti, G., Lavery, G., Nikkila, H., Palermo, M., Ricketts, M., McTernan, C., Bianchi, G., Manunta, P., Strazzullo, P., Mantero, F., White, P. C., and Stewart, P. M. (2000) *Hypertension* **36,** 187–194
27. Sharma, V. K., Rao, C. B., Sharma, A., Brahmachari, S. K., and Ramachandran, S. (2003) *Biomol. Struct. Dyn.* **21,** 303–310
28. Hui, J., Stangl, K., Lane, W. S., and Bindereif, A. (2003) *Nat. Struct. Biol.* **10,** 33–37
29. Hui, J., Reither, G., and Bindereif, A. (2003) *RNA (N. Y.)* **9,** 931–936
30. Bandyopadhyay, S., Sengupta, T. K., Fernandes, D. J., and Spicer, E. K. (2003) *Biochem. Pharmacol.* **66,** 1151–1162
31. Sengupta, T. K., Bandyopadhyay, S., Fernandes, D. J., and Spicer, E. K. (2004) *J. Biol. Chem.* **279,** 10855–10863
32. Guhaniyogi, J., and Brewer, G. (2001) *Gene (Amst.)* **265,** 11–23
33. Shih, S-C., and Claffey, K. P. (1999) *J. Biol. Chem.* **274,** 1359–1365

DECEMBER 2004 VOLUME 6 NO.12
www.nature.com/naturecellbiology

nature cell biology

Eps8 as an actin capper

Semaphorin signalling in reverse gear

A new ligase for p27^{Kip1}

nature
cell biology

Role of Bcl-2 family proteins in a non-apoptotic programmed cell death dependent on autophagy genes

Shigeomi Shimizu[1,2,3], Toku Kanaseki[4], Noboru Mizushima[4,5,6], Takeshi Mizuta[1,3], Satoko Arakawa-Kobayashi[4], Craig B. Thompson[7] and Yoshihide Tsujimoto[1,2,3,8]

Programmed cell death can be divided into several categories including type I (apoptosis) and type II (autophagic death)[1,2]. The Bcl-2 family of proteins are well-characterized regulators of apoptosis[3], and the multidomain pro-apoptotic members of this family, such as Bax and Bak, act as a mitochondrial gateway where a variety of apoptotic signals converge[4–6]. Although embryonic fibroblasts from Bax/Bak double knockout mice are resistant to apoptosis[4–6], we found that these cells still underwent a non-apoptotic death after death stimulation. Electron microscopic and biochemical studies revealed that double knockout cell death was associated with autophagosomes/autolysosomes. This non-apoptotic death of double knockout cells was suppressed by inhibitors of autophagy, including 3-methyl adenine, was dependent on autophagic proteins APG5 and Beclin 1 (capable of binding to Bcl-2/Bcl-x_L), and was also modulated by Bcl-x_L. These results indicate that the Bcl-2 family of proteins not only regulates apoptosis, but also controls non-apoptotic programmed cell death that depends on the autophagy genes.

It has been shown that cells lacking both Bax and Bak, the multidomain pro-apoptotic members of the Bcl-2 family, are completely resistant to apoptosis induced by various apoptotic stimuli, indicating that the multi-domain pro-apoptotic members act as a mitochondrial gateway for a variety of apoptotic signals[4–6]. However, although *Bax/Bak*$^{-/-}$ mice show several morphological abnormalities[4], programmed cell death seems to largely proceed in a normal manner, implying that a different mechanism compensates for apoptosis in these mice. Therefore, we investigated the response of cells from *Bax/Bak*$^{-/-}$ mice to various apoptotic stimuli in more detail.

When simian virus 40 (SV40)-transformed embryonic fibroblasts from *Bax/Bak*$^{-/-}$ mice (*Bax/Bak*$^{-/-}$ MEFs) were treated with etoposide (an inhibitor of topoisomerase II and a common apoptotic reagent), the cells became rounded, irregular and then ballooned (Fig. 1a; see Supplementary Information, Movie S1). We also continuously monitored these cells in the presence of propidium iodide (PI) (a membrane-impermeable stain for nucleic acids) under a fluorescent microscope. As shown in Fig. 1a, b and Supplementary Information, Movies S2 and S3, PI-positive cells were detected after 24 h and the majority of the cells were positively stained for PI by 48 h, indicating cell death. Note that the majority of PI-positive cells appeared to have been severely damaged. Consistently, when cell viability was assessed by the Resazurin reduction reaction using the Cell Titer Blue (CTB) assay, which measures the metabolic activity of viable cells in the same way as the MTT (methyl-thiazol-tetrazolium) assay, *Bax/Bak*$^{-/-}$ MEFs showed a significant decrease of viability (Fig. 1c). These results indicated that *Bax/Bak*$^{-/-}$ MEFs suffered a significant decrease of viability after etoposide treatment, although the extent of the change was smaller than in wild-type (WT) MEFs. As reported previously[4–6], etoposide-treated *Bax/Bak*$^{-/-}$ MEFs did not show any features of apoptosis (data not shown). Consistently, the addition of zVAD-fmk (a pan-caspase inhibitor) inhibited apoptosis of etoposide-treated WT MEFs, but did not improve the viability of *Bax/Bak*$^{-/-}$ MEFs (Fig. 1c).

To confirm the loss of cell viability after etoposide treatment, *Bax/Bak*$^{-/-}$ MEFs were exposed to etoposide, collected and re-cultured in standard medium. As shown in Fig. 1d, the proliferative activity of *Bax/Bak*$^{-/-}$ MEFs declined in a manner that was dependent on the duration of incubation with etoposide. Furthermore, the loss of cell viability was also confirmed by a clonogenicity (colony-forming) assay (Fig. 1e). Similar results were obtained when *Bax/Bak*$^{-/-}$ MEFs were treated with staurosporine (Fig. 1e and see Supplementary Information, Fig. S1a, b) or thapsigargin (data not shown). Moreover, etoposide and staurosporine induced a decrease of viability in primary *Bax/Bak*$^{-/-}$ MEFs and in thymocyte (see Supplementary Information, Fig. S1g, i, and data not shown). These results suggested that *Bax/Bak*$^{-/-}$ cells can be killed by various apoptosis-inducing reagents via a non-apoptotic process.

[1]Department of Post-Genomics & Diseases, Osaka University Medical School, [2]CREST and [3]SORST of the Japan Science and Technology Corporation (JST), 2-2 Yamadaoka, Suita, Osaka 565-0871, Japan. [4]Department of Cell Biology, National Institute for Basic Biology, and [5]PRESTO of the Japan Science and Technology Corporation (JST), Okazaki, Aichi 444-8585, Japan. [6]Department of Bioregulation and Metabolism, The Tokyo Metropolitan Institute of Medical Science, Tokyo 113-8613, Japan. [7]Departments of Medicine and Cancer Biology, Abramson Family Cancer Research Institute, University of Pennsylvania, Philadelphia, PA 19104 USA. [8]Correspondence should be addressed to: Y.T. (e-mail: tsujimot@gene.med.osaka-u.ac.jp)

Published online: 21 Novmeber 2004, DOI: 10.1038/ncb1192

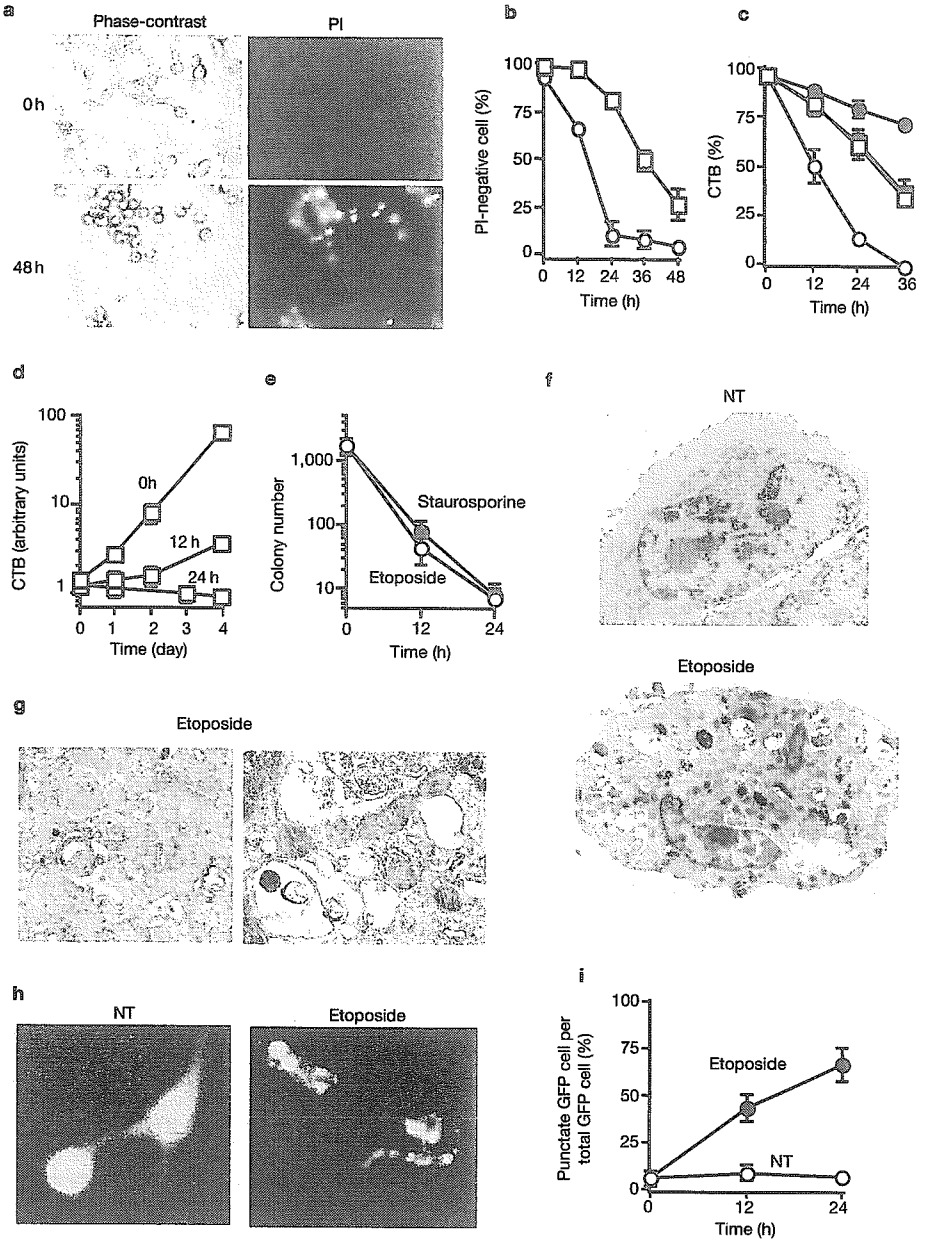

Figure 1 Loss of viability of and induction of autophagy in Bax/Bak$^{-/-}$ MEFs exposed to etoposide and staurosporine. (**a**) Representative photographs of Bax/Bak$^{-/-}$ MEFs treated with etoposide. Bax/Bak$^{-/-}$ MEFs were treated with 20 μM etoposide in the presence of PI (2 μM) for the indicated times, and were analysed under a phase-contrast and fluorescence (PI) microscope. (**b**, **c**) Reduced viability of Bax/Bak$^{-/-}$ MEFs after exposure to etoposide. WT (circles) and Bax/Bak$^{-/-}$ (squares) MEFs were treated with 20 μM etoposide in the presence (closed symbols) or absence (open symbols) of 100 μM zVAD-fmk. Then cell viability was measured by the PI staining (**b**) and CTB assay (**c**), and expressed as a percentage of the initial value without etoposide. Data are shown as mean ± s.d. ($n = 4$). (**d**) Reduced viability of etoposide-treated Bax/Bak$^{-/-}$ MEFs as assessed by proliferation assay. Bax/Bak$^{-/-}$ MEFs were either not treated (0 h) or were treated with 20 μM etoposide for 12 and 24 h, then all cells were recovered and 5,000 cells were reseeded. Viable cell numbers were measured on the indicated days by the CTB assay. Results were normalized by adjusting the day 0 value. $n = 4$. (**e**) Reduced viability of Bax/Bak$^{-/-}$ MEFs after exposure to etoposide and staurosporine, as assessed by clonogenicity assay. MEFs were treated with etoposide (20 μM) or staurosporine (1 μM) at the indicated times, collected, and 2,000 cells were seeded in the normal medium. After 1 week, colonies were counted. $n = 4$. (**f–i**) Induction of autophagy in Bax/Bak$^{-/-}$ MEFs by etoposide. (**f**) Electron micrograph (×14,800) of Bax/Bak$^{-/-}$ MEF treated with etoposide (20 μM) for 18 h. Representative features of Bax/Bak$^{-/-}$ MEFs that have received no treatment (NT; that is, are healthy) are also shown (NT: ×14,000). (**g**) In magnified photographs, a large number of autolysosomes/autophagosomes (left: ×26,000) were observed, but the mitochondria were unaffected (right: ×17,000). (**h**, **i**) Punctate GFP–LC3 fluorescence in Bax/Bak$^{-/-}$ MEFs treated with etoposide. GFP–LC3-transfected cells were incubated with and without etoposide (20 μM) for 24 h (**h**) or the indicated times (**i**), and then examined by fluorescent microscopy. (**h**) Representative photographs of healthy (NT) and etoposide-treated Bax/Bak$^{-/-}$ MEFs are shown. (**i**) The percentage of cells with punctate GFP–LC3 fluorescence was calculated relative to all GFP-positive cells. Data are shown as mean ± s.d. ($n = 4$).

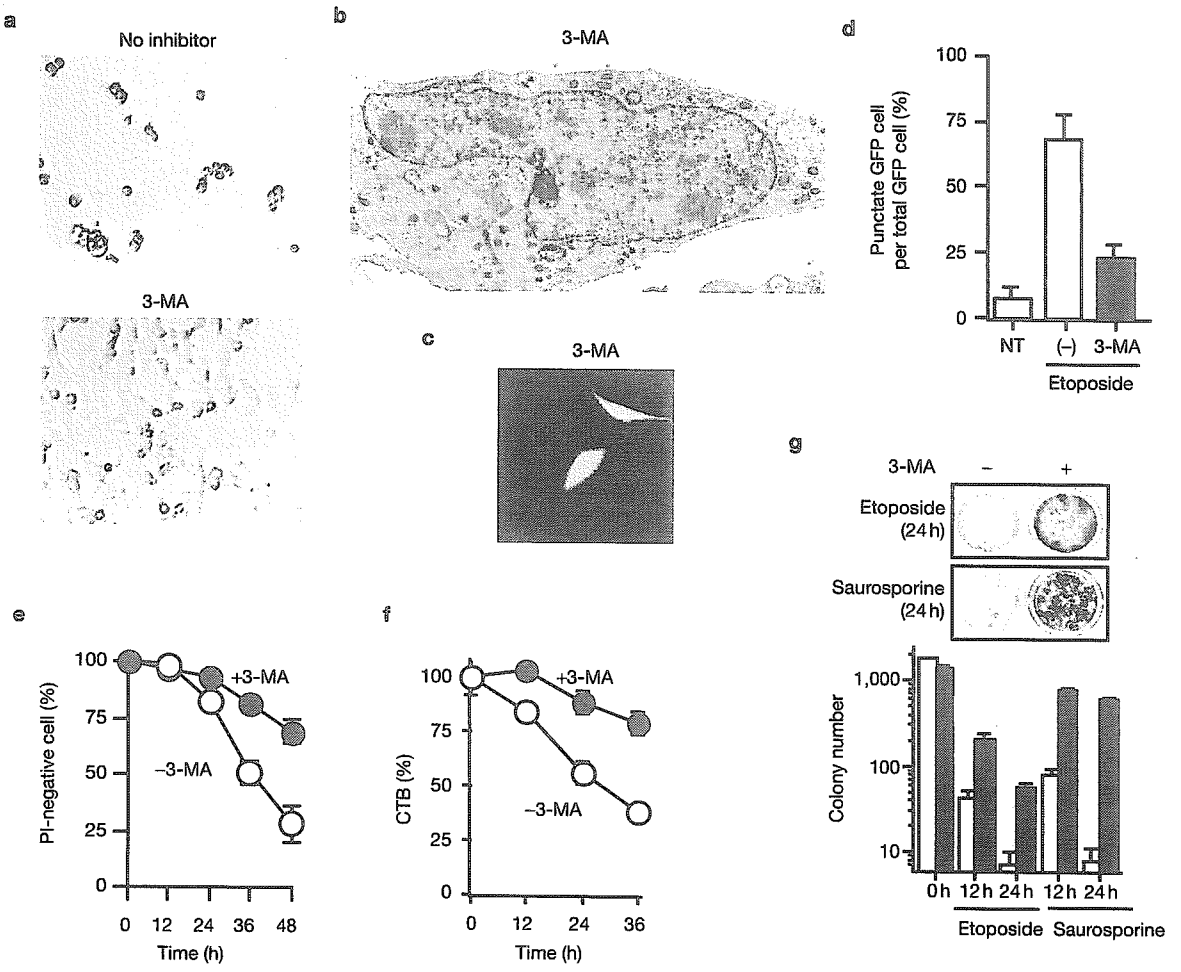

Figure 2 Inhibition of etoposide-induced death of Bax/Bak$^{-/-}$ MEFs by 3-MA. (**a**, **b**) Bax/Bak$^{-/-}$ MEFs were treated with 20 μM etoposide in the absence or presence of 10 mM 3-MA for 24 h, and then were examined by phase-contrast microscopy (**a**) and electron microscopy (×8,400) (**b**). Autolysosomes/autophagosomes were hardly observed. (**c**, **d**) Reduction of punctate GFP–LC3 fluorescence in Bax/Bak$^{-/-}$ MEFs by 3-MA. Bax/Bak$^{-/-}$ MEFs that were transfected with GFP–LC3 were incubated without (NT) or with 20 μM etoposide in the presence or absence of 10 mM 3-MA for 24 h, and then were examined by confocal fluorescent microscopy. (**c**) Representative photograph of etoposide-treated Bax/Bak$^{-/-}$ MEFs in the presence of 3-MA. (**d**) The percentage of cells with punctate GFP–LC3 fluorescence was calculated relative to all GFP–LC3-positive cells. Data are shown as mean ± s. d. ($n = 4$). (**e**–**g**) Inhibition of etoposide- and staurosporine-induced cell death by 3-MA. Bax/Bak$^{-/-}$ MEFs were treated with 20 μM etoposide (**e**–**g**) or 1 μM staurosporine (**g**) in the absence (open symbols) or presence (closed symbols) of 10 mM 3-MA for the indicated time. Cell viability was measured by PI staining (**e**), CTB assay (**f**) and clonogenicity assay (**g**) (as in Fig. 1e). Upper panels in **g**: viable cells were visualized by staining with calcein-AM. $n = 4$.

To investigate the mechanism underlying the death of *Bax/Bak*$^{-/-}$ MEFs induced by apoptotic stimuli, the cells were examined by electron microscopy. As shown in Fig. 1f, g, the majority of etoposide-treated *Bax/Bak*$^{-/-}$ MEFs, but not healthy MEFs, contained a number of autophagosomes/autolysosomes, which are a characteristic feature of autophagy. Moreover, a significant number of cells appeared to have undergone destruction by abundant autophagosomes/autolysosomes, raising the possibility that an autophagic process might be involved in the non-apoptotic death of *Bax/Bak*$^{-/-}$ MEFs. In contrast, many of the mitochondria appeared normal (Fig. 1g), although some were found inside the autophagosomes (data not shown). Although the nuclei were deformed, neither chromatin condensation nor nuclear fragmentation was observed (Fig. 1f), confirming the absence of apoptotic cell death. Autophagy is a pathway for the bulk degradation of subcellular constituents through the creation of autophagosomes/autolysosomes in response to stresses such as nutrient deprivation[7]. In general, autophagy is utilized so that cells can survive, but constitutive activation of autophagy may induce cell death. To visualize autophagy, green fluorescent protein (GFP)-tagged light-chain 3 (LC3) (ref. 8) was expressed in *Bax/Bak*$^{-/-}$ MEFs. During the autophagic process, LC3 is concentrated in autophagosomes, so the punctate fluorescence produced by GFP–LC3 can be used as a good indicator of autophagy[8]. As shown in Fig. 1h, diffuse cytoplasmic localization of GFP–LC3 was observed in healthy *Bax/Bak*$^{-/-}$ MEFs, whereas etoposide-treated *Bax/Bak*$^{-/-}$ MEFs showed punctuate fluorescence. The number of cells with punctate GFP–LC3 fluorescence increased in a time-dependent manner after etoposide treatment (Fig. 1i). Similar findings were also observed when *Bax/Bak*$^{-/-}$ MEFs were treated with staurosporine (see Supplementary Information, Fig. S1c, d). All of these results indicated that apoptotic stimuli could induce non-apoptotic death of *Bax/Bak*$^{-/-}$ MEFs, which was associated with the generation of autophagosomes/autolysosomes.

To elucidate the involvement of the autophagic process in non-apoptotic death of *Bax/Bak*$^{-/-}$ MEFs, the effects of several inhibitors of autophagy were tested. Autophagy is known to be inhibited by PI3 kinase inhibitors,

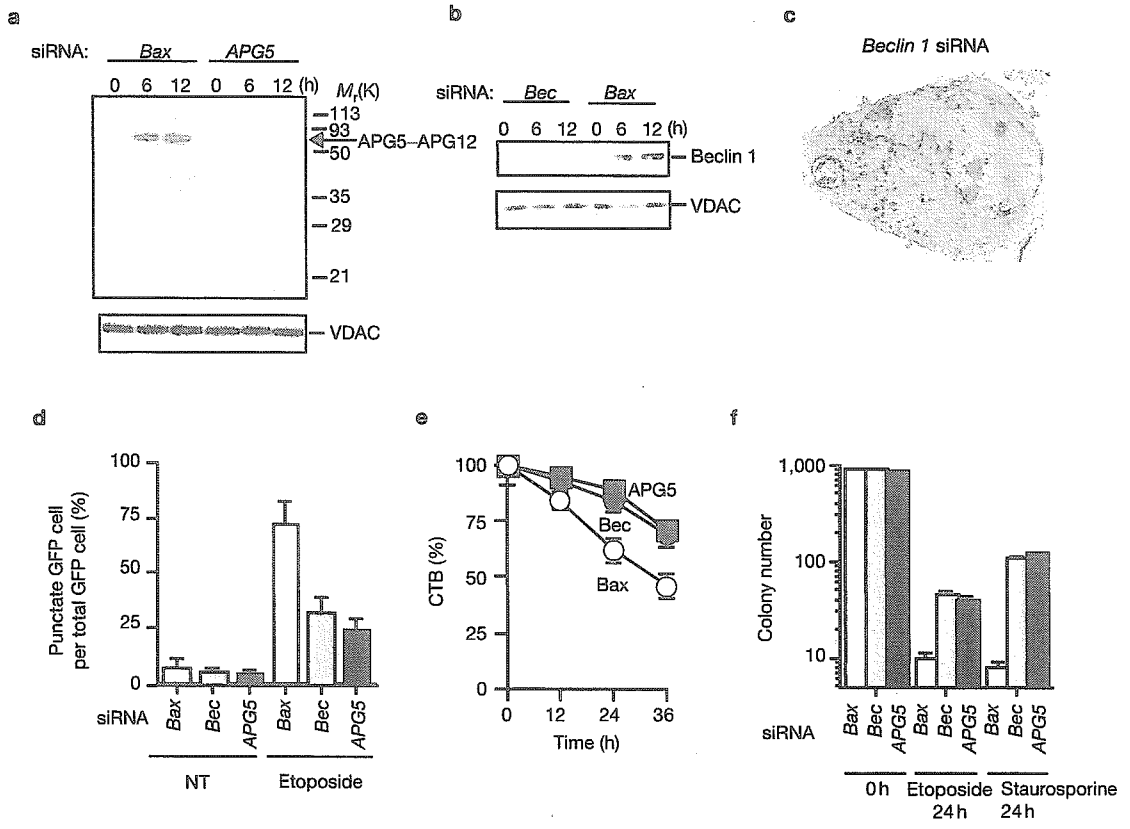

Figure 3 Inhibition of etoposide-induced death of Bax/Bak$^{-/-}$ MEFs by silencing autophagy genes. (**a**, **b**) Bax/Bak$^{-/-}$ MEFs were treated with the indicated siRNAs (10 μg) for 24 h and then incubated with 20 μM etoposide for the indicated times. Expression of APG5–APG12 complex (**a**), Beclin 1 (**b**) and VDAC (loading control) was analysed by Western blot analysis. (**c**) Inhibition of etoposide-induced autophagy by silencing of Beclin 1. Bax/Bak$^{-/-}$ MEFs with silencing of Beclin 1 were treated with 20 μM etoposide at 18 h and were analysed by electron microscopy (×8,500). (**d**) Reduction of punctate GFP–LC3 fluorescence in Bax/Bak$^{-/-}$ MEFs by silencing of Beclin 1 and APG5. Bax/Bak$^{-/-}$ MEFs that were transfected with GFP–LC3 together with the indicated siRNAs, were incubated without (NT) or with 20 μM etoposide for 24 h, and then examined by confocal fluorescent microscopy. The percentage of cells with punctate GFP–LC3 fluorescence was calculated relative to all GFP–LC3-positive cells. Data are shown as mean ± s.d. ($n = 4$). (**e**, **f**) Inhibition of etoposide- and staurosporine-induced cell death by silencing of Beclin 1 and APG5. Bax/Bak$^{-/-}$ MEFs that were treated with the indicated siRNAs were incubated with 20 μM etoposide (**e**, **f**) or 1 μM staurosporine (**f**) for the indicated time. Cell viability was measured by CTB assay (**e**) and clonogenicity assay (**f**). $n = 4$.

such as 3-methyladenine (3-MA) and wortmannin[7]. When *Bax/Bak*$^{-/-}$ MEFs were treated with etoposide in the presence of 3-MA, cell rounding and detachment were almost completely inhibited (Fig. 2a). Etoposide-induced development of autophagosomes/autolysosomes was also inhibited by 3-MA (Fig. 2b–d). Cell viability was markedly improved by 3-MA, as shown by PI staining (Fig. 2e; see Supplementary Information, Movies S4 and S5), the CTB assay (Fig. 2f) and a clonogenicity assay (Fig. 2g). Similar results were obtained with wortmannin (data not shown). Note that incubation with 3-MA or wortmannin showed only slight toxicity to cells (5–10% reduction of cell viability in 24 h). Because we used low concentrations of these drugs for all subsequent studies, toxicity should not be an issue. 3-MA also inhibited staurosporine-induced death of *Bax/Bak*$^{-/-}$ MEFs (Fig. 2g and see Supplementary Information, Fig. S1e, f), and non-apoptotic death induced by etoposide and staurosporine in primary *Bax/Bak*$^{-/-}$ MEFs and thymocytes (see Supplementary Information, Fig. S1h, i, and data not shown).

For further confirmation of the involvement of an autophagic process in the non-apoptotic death of *Bax/Bak*$^{-/-}$ MEFs, we used gene silencing with short interfering RNA (siRNA) to inhibit some genes related to the autophagic process. The protein APG5 is essential for the generation of autophagosomes by covalent binding to APG12 (ref. 9). Beclin 1 is part of a class III PI3 kinase complex that is also crucial for autophagy[10], and may function upstream of other APG proteins[11]. Interestingly, when *Bax/Bak*$^{-/-}$ MEFs were treated with etoposide, there was considerable accumulation of both the APG5–APG12 complex and Beclin 1 (Fig. 3a, b), consistent with induction of the autophagic process in etoposide-treated *Bax/Bak*$^{-/-}$ MEFs. Accumulation of Beclin 1 and the APG5–APG12 complex was inhibited by silencing of the respective genes (Fig. 3a, b). We used *Bax* siRNA as a control because Bax was absent in *Bax/Bak*$^{-/-}$ MEFs. Etoposide-induced generation of autophagosomes/autolysosomes was markedly inhibited by silencing of Beclin 1 and APG5 (Fig. 3c, d, and data not shown). Silencing of Beclin 1 and APG5 reduced the etoposide-induced death of *Bax/Bak*$^{-/-}$ MEFs (Fig. 3e, f). Similar results were obtained when cells were treated with staurosporine (Fig. 3f). All of these findings indicated that various apoptotic stimuli could induce non-apoptotic death of *Bax/Bak*$^{-/-}$ MEFs, which was dependent on autophagy genes.

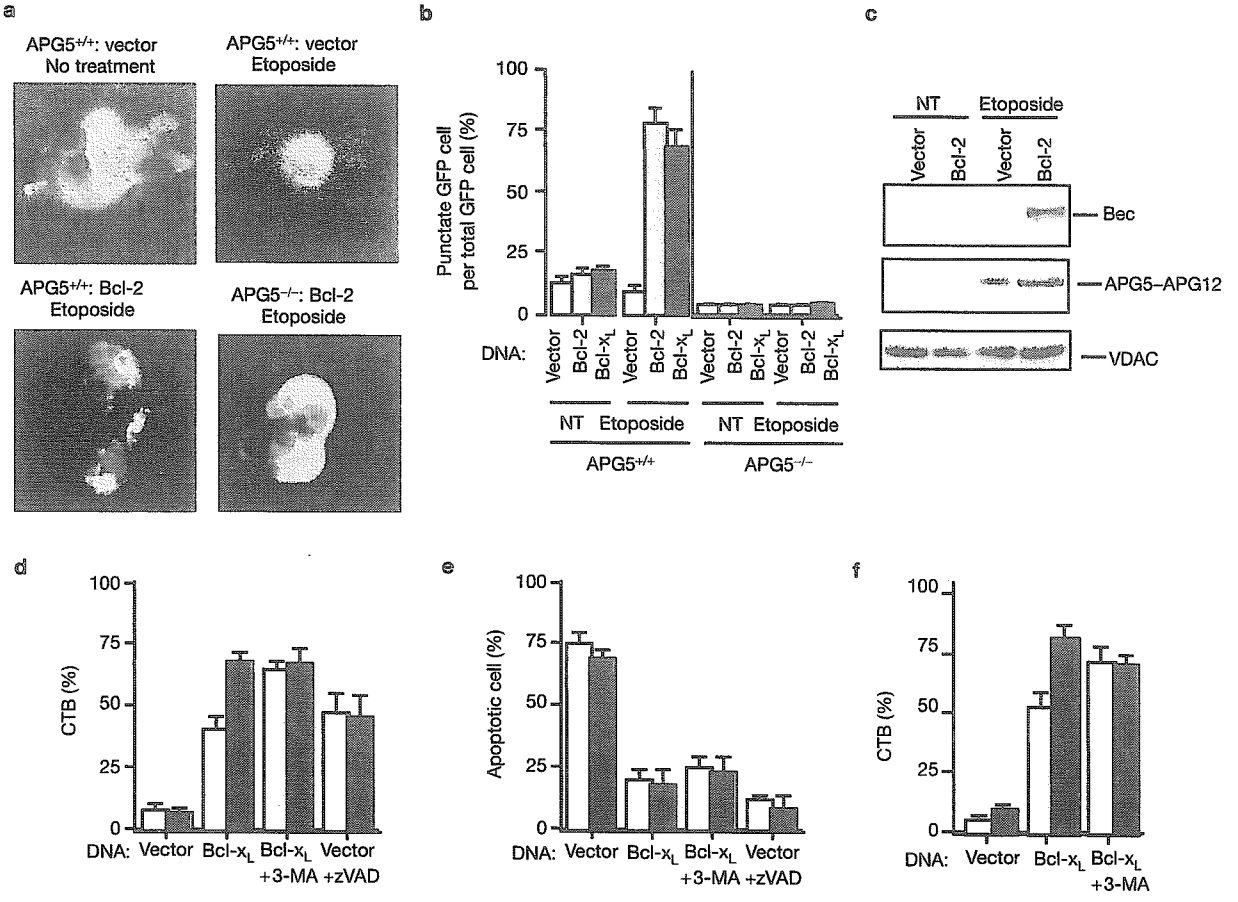

Figure 4 Occurrence of etoposide-induced, 3-MA-inhibitable, non-apoptotic death in MEFs by overexpressed Bcl-2/Bcl-x_L. (**a**, **b**) APG5-dependent punctate GFP–LC3 fluorescence in Bcl-2-transfected MEFs after etoposide treatment. $APG5^{+/+}$ and $APG5^{-/-}$ MEFs that were transfected with both GFP–LC3 and the indicated plasmids (Bcl-2 or vector) were incubated without or with 20 μM etoposide for 24 h, then examined by confocal fluorescent microscopy (**a**). The percentage of cells with punctate GFP–LC3 fluorescence was calculated relative to all GFP–LC3-positive cells (**b**). (**c**) Accumulation of Beclin 1 and APG5–APG12 complex in Bcl-2-transfected MEFs after etoposide treatment. WT MEFs were transfected with the indicated plasmids, and were incubated without (NT) or with 20 μM etoposide for 24 h. (**d**, **e**) Occurrence of etoposide-induced 3-MA-inhibitable non-apoptotic death in Bcl-x_L-overexpressing $APG5^{+/+}$ MEFs, but not $APG5^{-/-}$ MEFs. $APG5^{+/+}$ (open columns) and $APG5^{-/-}$ (closed columns) MEFs were transfected with the indicated plasmids (2 μg). After 24 h, transfected cells were incubated with 20 μM of etoposide in the presence or absence of 100 μM of zVAD or 10 mM of 3-MA for 24 h, and cell viability was measured by the CTB assay (**d**) and apoptotic nuclear morphology (**e**). Data are shown as mean ± s.d. ($n = 4$). (**f**) Overexpression of Bcl-x_L does not sensitize Beclin 1-silenced MEFs to etoposide-induced 3-MA-inhibitable non-apoptotic death. WT MEFs with silencing of control GFP (open columns) or Beclin 1 (closed columns) were transfected with the indicated plasmids (1 μg). After 24 h, transfected cells were incubated with 20 μM of etoposide in the presence or absence of 10 mM of 3-MA for 24 h, and cell viability was measured by the CTB assay. $n = 3$.

To confirm that apoptotic stimulation induced non-apoptotic cell death in *Bax/Bak*$^{-/-}$ MEFs owing to the absence of Bax and Bak, either Bax or Bak was expressed in these cells and then treatment with etoposide was performed. In contrast to *Bax/Bak*$^{-/-}$ MEFs, Bax- (or Bak)-transfected *Bax/Bak*$^{-/-}$ MEFs developed certain features of apoptosis, and were inhibited by zVAD-fmk, but not by 3-MA (see Supplementary Information, Fig. S2a, b). Thus, etoposide-induced non-apoptotic death of *Bax/Bak*$^{-/-}$ MEFs was a consequence of the inhibition of Bax/Bak activity.

To show that non-apoptotic death was not a simple consequence of the inhibition of apoptosis, we next examined non-apoptotic death in zVAD-added WT MEFs, and Apaf-1- and caspase-9-deficient MEFs after treatment with etoposide. In all cases, a small (but significant) decrease of cell viability was detected, but this decrease was not inhibited by 3-MA (see Supplementary Information, Fig. S2c–f). Furthermore, etoposide-treated WT MEFs showed only mild autophagic manifestations (see Supplementary Information, Fig. S2g–i), indicating that the 3-MA-inhibitable non-apoptotic death of *Bax/Bak*$^{-/-}$ MEFs was not merely due to inhibition of apoptosis, but was related to deficiency of both Bax and Bak.

We next examined the effect of overexpression of Bcl-2 and Bcl-x_L in WT MEFs. These cells were expected to undergo 3-MA-inhibitable non-apoptotic death, as do *Bax/Bak*$^{-/-}$ MEFs in response to apoptotic stimulations. MEFs overexpressing Bcl-2 (and also Bcl-x_L) showed punctuate GFP–LC3 fluorescence (Fig. 4a, b) and greater accumulation of Beclin 1 and APG5–APG12 complex after etoposide treatment than did WT MEFs (Fig. 4c). This punctuate GFP–LC3 fluorescence was not observed in *APG5*$^{-/-}$ MEFs (Fig. 4a, b), in which autophagy was impaired[18], indicating that overexpression of Bcl-2/Bcl-x_L induced APG5-dependent autophagy in WT MEFs after etoposide treatment. To confirm that cells overexpressing Bcl-2/Bcl-x_L undergo etoposide-induced non-apoptotic death, *APG5*$^{-/-}$ MEFs were transfected with a

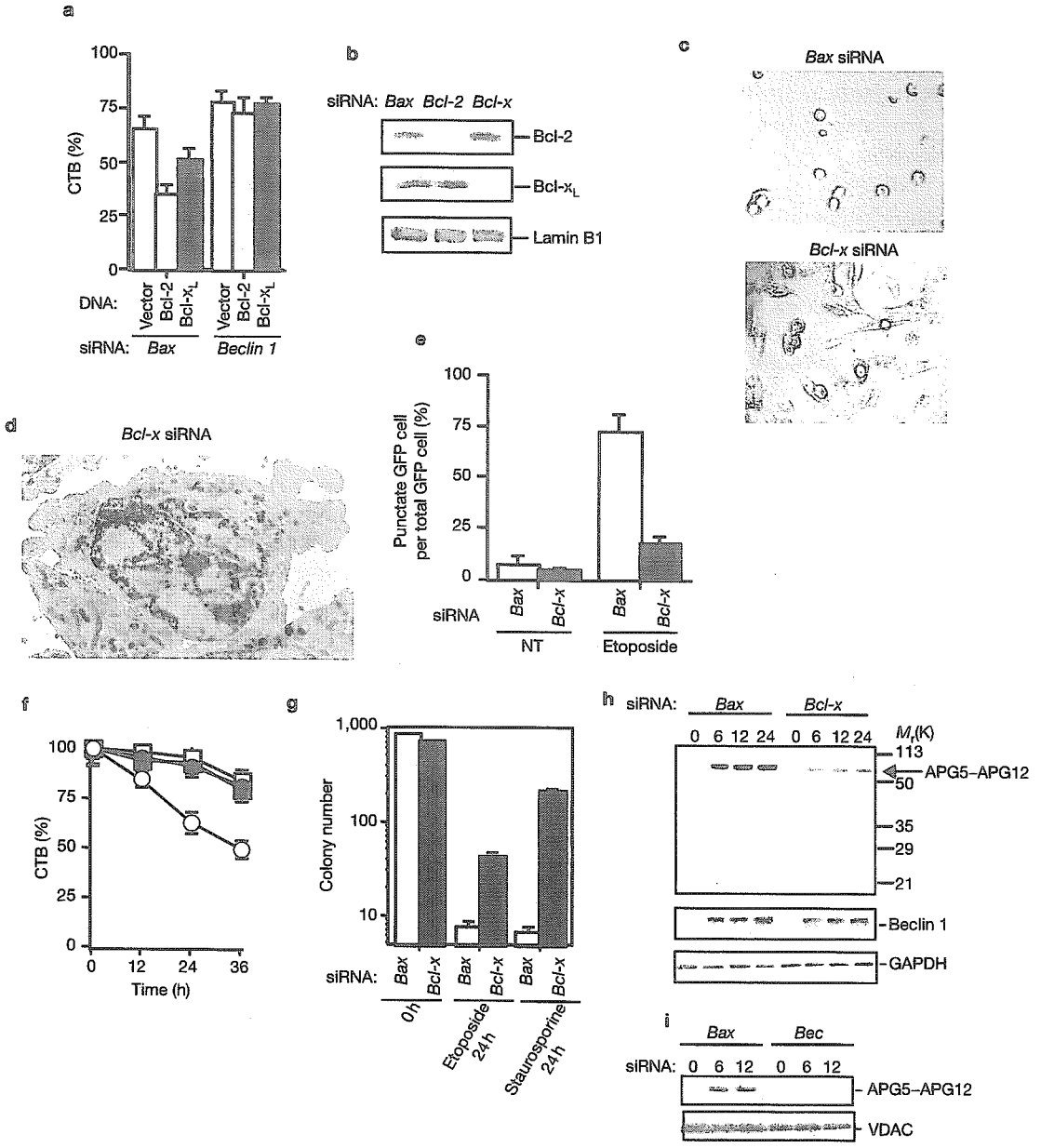

Figure 5 Inhibition of non-apoptotic death in etoposide-treated Bax/Bak$^{-/-}$ MEFs by siRNA for Bcl-x. (**a**) Enhancement of etoposide-induced non-apoptotic death by overexpression of human Bcl-2 and Bcl-x$_L$ in Bax/Bak$^{-/-}$ MEFs in a Beclin 1-dependent manner. Bax/Bak$^{-/-}$ MEFs with silencing of control Bax or Beclin 1 were transfected with the indicated plasmids (1 μg). After 24 h, the transfected cells were incubated with 20 μM etoposide for 24 h, and cell viability was assessed by the CTB assay. Data are shown as mean ± s.d. ($n = 3$). (**b**) Bax/Bak$^{-/-}$ MEFs were transiently transfected with 10 μg of siRNA for Bcl-2, Bcl-x, or Bax (negative control) for 24 h. Expression levels of Bcl-2, Bcl-x$_L$ and Lamin B (loading control) were analysed by Western blot analysis. (**c–e**) Inhibition of etoposide-induced autophagy in Bax/Bak$^{-/-}$ cells treated with siRNA for Bcl-x. (**c**) Bax/Bak$^{-/-}$ MEFs that were transfected with the indicated siRNAs were treated with 20 μM etoposide for 24 h, then examined by phase-contrast microscopy. (**d**) Bax/Bak$^{-/-}$ MEFs that were transfected with siRNA for Bcl-x and then treated with etoposide for 18 h were analysed by electron microscopy (×8,500). (**e**) Reduction of punctate GFP–LC3 fluorescence in etoposide-treated Bax/Bak$^{-/-}$ MEFs by silencing of Bcl-x. Bax/Bak$^{-/-}$ MEFs that were transfected with both GFP–LC3 and the indicated siRNAs were incubated without (NT) or with etoposide for 24 h, and then were examined by confocal fluorescent microscopy. The percentage of cells with punctate GFP–LC3 fluorescence was calculated relative to all GFP–LC3-positive cells. $n = 4$. (**f**) Inhibition of etoposide-induced cell death by silencing of Bcl-x. Bax/Bak$^{-/-}$ MEFs were transfected with siRNA (circles, siRNA for Bax; squares, siRNA for Bcl-x) were treated with 20 μM etoposide in the absence (open symbols) or presence (closed symbols) of 10 mM 3-MA, and cell viability was assessed by the CTB assay at the indicated times. $n = 4$. (**g**) Clonogenicity assay of Bax/Bak$^{-/-}$ MEFs after exposure to etoposide and staurosporine. Bax/Bak$^{-/-}$ MEFs that were transfected with the indicated siRNAs were treated with 20 μM etoposide or 1 μM staurosporine at 24 h. After collection, 2,000 cells were seeded in the normal medium. After one week, colonies were counted. (**h, i**) Inhibition of APG5–APG12 induction by silencing of Bcl-x or Beclin 1. Bax/Bak$^{-/-}$ MEFs were treated with the indicated siRNAs (10 μg) for 24 h and then incubated with 20 μM etoposide for the indicated times. Expression of APG5–APG12 complex, Beclin 1 and GAPDH/VDAC (loading control) was analysed by Western blot analysis.

Bcl-x_L-expressing plasmid and then treated with etoposide. As shown in Fig. 4d, the viability of Bcl-x_L-expressing *APG5*$^{-/-}$ MEFs was superior to that of Bcl-x_L-expressing *APG5*$^{+/+}$ MEFs, and the latter was increased by 3-MA. In both types of cells, apoptosis was similarly inhibited (Fig. 4e). Thus, whereas overexpression of Bcl-x_L clearly increased the survival of both *APG5*$^{+/+}$ and *APG5*$^{-/-}$ cells, Bcl-x_L overexpression increased the difference in cell death between *APG5*$^{+/+}$ and *APG5*$^{-/-}$ cells, which would be predicted to be the autophagic component. In contrast to Bcl-x_L, vector DNA transfection did not produce any difference between the viability of *APG5*$^{-/-}$ MEFs and *APG5*$^{+/+}$ MEFs, irrespective of the presence of zVAD-fmk (Fig. 4d). Similar findings were obtained when Bcl-2-expressing plasmid was used (data not shown). Non-apoptotic death observed in MEFs with overexpressed Bcl-2/Bcl-x_L was not seen when Beclin 1 was silenced (Fig. 4f). These data suggested that overexpression of Bcl-2 or Bcl-x_L not only inhibited apoptosis, but also sensitized at least a fraction of cells to non-apoptotic death dependent on autophagy genes (such as Bax/Bak-deficiency); however, we could not formally exclude the possibility that overexpression of Bcl-2 and Bcl-x_L simply increases the efficiency of autophagosome formation, which may not necessarily be translated into more cell death, and that APG5 and Beclin 1 are relevant modulators of cell death.

In the *Bax/Bak*$^{-/-}$ cells, apoptotic reagents induced non-apoptotic cell death, which was dependent on genes related to autophagy, including Beclin 1. Beclin 1 interacts with Bcl-2/Bcl-x_L (but not Bax/Bak)[12], raising the possibility that Bcl-2/Bcl-x_L may have a role in the non-apoptotic death of *Bax/Bak*$^{-/-}$ MEFs. We first examined the effect of overexpression of Bcl-2 and Bcl-x_L in *Bax/Bak*$^{-/-}$ MEFs. As expected, overexpression of Bcl-2 and Bcl-x_L in *Bax/Bak*$^{-/-}$ MEFs resulted in enhancement of the non-apoptotic death, which was cancelled by silencing of Beclin 1 (Fig. 5a). We next examined the effect of silencing these molecules in *Bax/Bak*$^{-/-}$ MEFs by using siRNA. Endogenous Bcl-2 and Bcl-x_L were almost completely eliminated from *Bax/Bak*$^{-/-}$ MEFs by the respective siRNAs (Fig. 5b). Despite etoposide treatment, a large fraction of the Bcl-x-silenced *Bax/Bak*$^{-/-}$ MEFs appeared healthy (Fig. 5c) and the creation of autophagosomes was markedly suppressed (Fig. 5d, e). The majority of the cells remained viable irrespective of the addition of 3-MA (Fig. 5f), indicating that the non-apoptotic death was not induced and suggesting that Bcl-x_L was required for the non-apoptotic death of *Bax/Bak*$^{-/-}$ MEFs. As expected in the absence of Bax/Bak, these cells did not undergo apoptotic death (data not shown). In contrast to the silencing of Bcl-x, silencing of Bcl-2 did not have any effect (see Supplementary Information, Fig. S2j, k)—probably not owing to functional differences between Bcl-2 and Bcl-x, but to the much lower level of Bcl-2 than Bcl-x_L expression in MEFs—because Bcl-2 overexpression cancelled the effect of Bcl-x silencing (see Supplementary Information, Fig. S2l). The improved viability after Bcl-x silencing was also confirmed by a clonogenicity assay (Fig. 5g). As shown in Fig. 5h, the etoposide-induced increase of Beclin 1 in Bcl-x-silenced *Bax/Bak*$^{-/-}$ MEFs was similar to that in control *Bax/Bak*$^{-/-}$ MEFs, whereas induction of APG5–APG12 was far weaker in Bcl-x-silenced *Bax/Bak*$^{-/-}$ MEFs than in control *Bax/Bak*$^{-/-}$ MEFs. Because Beclin 1 binds to Bcl-x_L, and silencing of Beclin 1 reduced the APG5–APG12 level (Fig. 5i), Bcl-x_L might be required for induction of APG5–APG12 through regulation of Beclin 1.

Because *Bax/Bak*$^{-/-}$ MEFs lost viability after exposure to apoptotic stimuli in an autophagic protein-dependent and 3-MA-inhibitable manner, it might be assumed that this type of non-apoptotic death is similar to death induced by nutrient starvation, which also activates the autophagic process. However, etoposide/staurosporine-induced non-apoptotic death of *Bax/Bak*$^{-/-}$ cells showed substantial differences from death induced by amino-acid starvation on the basis of the following findings: (1) whereas etoposide/staurosporine-induced non-apoptotic death of *Bax/Bak*$^{-/-}$ is inhibited by 3-MA, amino-acid starvation-induced death is not inhibited, but rather is enhanced by 3-MA (see Supplementary Information, Fig. S3a, b), probably owing to an impaired supply of amino acids; (2) amino-acid starvation induces apoptosis in WT cells that are dependent on Bax/Bak (see Supplementary Information, Fig. S3b); and (3) accumulation of Beclin 1 and APG5–APG12 was observed in cells undergoing etoposide/staurosporine-induced non-apoptotic death, but not in cells that died of amino-acid starvation (see Supplementary Information, Fig. S3c). Thus, the non-apoptotic death of *Bax/Bak*$^{-/-}$ MEFs occurs in a different manner from starvation-induced cell death. Furthermore, although autophagic proteins are required, their role shows considerable differences between nutrient starvation and non-apoptotic death of *Bax/Bak*$^{-/-}$ cells.

Non-apoptotic (type II-like) death was observed in *Bax/Bak*$^{-/-}$ MEFs irrespective of their immortalization and was also seen in *Bax/Bak*$^{-/-}$ thymocytes. However, whether other normal cells also have the potential to undergo type II-like death requires further investigation. Among the cultured cell lines tested so far, overexpression of Bcl-2 did not sensitize HeLa, Jurkat or HCT116 cells to etoposide-induced non-apoptotic death (data not shown). Non-apoptotic death potential could be restricted to certain cells in the *in vitro* setting. As previously suggested[10], many cancer cells might have lost the ability to undergo non-apoptotic death as a growth advantage.

How does the Bcl-2 family of proteins regulate the non-apoptotic death? Overexpression of proteins in the BH (Bcl-2 homology) 3 subfamily (BH3-only proteins) did not induce the non-apoptotic death in *Bax/Bak*$^{-/-}$ MEFs (see Supplementary Information, Fig. S4), indicating that activation of BH3-only proteins is not sufficient to produce this form of cell death. Because Beclin 1 is required for the non-apoptotic death of *Bax/Bak*$^{-/-}$ cells and because Bcl-2/Bcl-x_L (but not Bax/Bak) binds to Beclin 1 (ref. 12), Bcl-2/Bcl-x_L might influence the creation of autophagosomes at least partly by regulation of Beclin 1. This notion is supported by the fact that the apoptotic stimulus-dependent increase of APG5–APG12 in *Bax/Bak*$^{-/-}$ MEFs (which was regulated by Beclin 1) was markedly reduced by silencing Bcl-x. This hypothesis certainly needs to be tested by using mutants of Bcl-2/Bcl-x_L and Beclin 1 that fail to interact with each other.

Anti-apoptotic Bcl-2/Bcl-x_L and pro-apoptotic Bax/Bak regulate apoptosis in opposite directions by acting on each other as well as by influencing other molecules, so the balance between these proteins is a crucial determinant of whether or not apoptosis occurs[3]. The fact that *Bax/Bak*$^{-/-}$ MEFs, in which anti-apoptotic Bcl-2 family members dominate over pro-apoptotic members, and Bcl-2/Bcl-x_L-overexpressing MEFs undergo the non-apoptotic death, suggests that the balance between Bcl-2/Bcl-x_L and Bax/Bak is also crucial for determining the occurrence of the non-apoptotic death. It has previously been described that some Bcl-2 family members can reverse their death-regulating activities, depending on expression levels or cellular contexts[13–16]. Overexpression of Bcl-2 has been reported to promote cell death from different mechanisms, for example, via proteolytic cleavage with caspases[15] or via interaction with an orphan nuclear receptor Nur77 (ref. 16). Therefore, the possibility was not formally excluded that an important role of Bcl-2/Bcl-x_L in the non-apoptotic death is dependent on this cryptic pro-death activity.

In conclusion, these findings demonstrate a previously unknown role of the Bcl-2 family in the regulation of non-apoptotic (type II-like) programmed cell death, in addition to the well-known role of this protein family in apoptosis. □

METHODS

Antibodies and chemicals. Anti-mouse Bcl-2, anti-Beclin 1 and anti-GAPDH (6G7) monoclonal antibodies were obtained from BD Biosciences (San Jose, CA). Anti-Lamin B1 and anti-VDAC monoclonal antibodies were purchased from Zymed (San Francisco, CA) and Calbiochem (La Jolla, CA), respectively. Anti-Bcl-x (L-19) polyclonal antibody was obtained from Santacruz Biotechnology (Santa Cruz, CA). Anti-APG5 polyclonal antibody was described previously[9]. 3-MA and Cell Titer Blue were obtained from ICN Biochemicals (Irvine, CA) and Promega (Madison, WI), respectively. Other chemicals were purchased from Wako (Osaka, Japan).

Cell culture and DNA transfection. Primary and SV40 T antigen-transformed WT and *Bax/Bak*$^{-/-}$ MEFs were grown in Dulbecco's modified Eagle's medium (DMEM). Apaf-1-deficient and caspase-9-deficient MEFs and their control MEFs (provided by X. Wang and K. Kuida, respectively) were also grown in the same medium. DNAs encoding human Bax, human Bak, human Bcl-2 and human Bcl-x_L in the pUC-CAGGS expression vector[17] were used. The GFP–LC3 expression construct was described elsewhere[8]. Cells (1×10^6) were transfected with plasmid DNA using the Amaxa electroporation system according to the supplier's protocol (kit V, program U-20). The transfection efficiency was more than 75% as assessed by co-transfection with DNA expressing GFP. All the siRNAs were produced by Dharmacon Research. The sequences used were as follows (numbers in parentheses indicate nucleotide positions within the respective open reading frame): mouse *Bcl-x* siRNA, 5′-AAGGAUACAGCUGGAGUCAGU-3′ (59–79); mouse *Bcl-2* siRNA, 5′-AAGUACAUACAUUAUAAGCUG-3′ (49–69); mouse *Bax* siRNA, 5′-AACAGAUCAUGAAGACAGGGG-3′ (50–70); mouse *Beclin 1* siRNA, 5′-AAGAUCCUGGACCGGGUCACC-3′ (91–111); mouse *APG5* siRNA, 5′-AACUUGCUUUACUCUCUCUAUCA-3′ (51–71). Cells (1×10^6) were transfected with 10 μg of siRNA using the Amaxa electroporation system. In the case of transfection with complementary DNA and siRNA, cDNAs (1 μg) were transfected, and after 24 h siRNAs (10 μg) were introduced.

Cell viability assay. Cells (3.5×10^6 per well) were seeded into 6-well dishes. After 24 h, the cells were treated with etoposide (20 μM) or staurosporine (1 μM) in the presence or absence of zVAD-fmk (100 μM) or 3-MA (10 mM). PI (2 μM) was added into the medium, and cells were observed under a BX50 fluorescence microscope (Olympus, Tokyo, Japan). In another experiments, all of the cells, including floating cells, were collected and viability was assessed by nuclear morphology after Hoechst 33342 (Ho342) staining, or the CTB assay. Briefly, cells were stained with 1 μM Ho342 for 5 min at room temperature, and were analysed with a fluorescence microscope (Olympus, BX50). The CTB assays were performed using CTB assay reagent, according to the supplier's protocols.

To examine the proliferation ability, MEFs were treated with etoposide or staurosporine, all the cells were recovered and 5,000 or 10,000 cells were re-cultured in standard medium into 96-well or 48-well dishes, respectively. Viable cell numbers were measured on the indicated days by the CTB assay. In the clonogenicity assay, MEFs were treated with etoposide or staurosporine, collected, and 2,000 cells were seeded in standard medium into 24-well dishes. After one week, colony numbers were counted.

Staining of autophagosomes. Cells were transfected with 1 μg of GFP–LC3 expression plasmid[8]. After 24 h, cells were treated with etoposide or staurosporine, and the fluorescence of GFP–LC3 was observed under a confocal fluorescence microscope (LSM 510 META, Zeiss, Thornwood, NY).

Electron microscopy. Cells were fixed with 2% paraformaldehyde/2% glutaraldehyde in 0.1 M phosphate buffer (pH 7.4), followed by 1% OsO_4. After dehydration, thin sections were stained with uranyl acetate and lead citrate for observation under a JEM 100 CX electron microscope (JEOL, Peabody, MA).

Note: Supplementary Information, Information is available on the Nature Cell Biology website.

ACKNOWLEDGEMENTS

We are grateful to S. J. Korsmeyer for providing SV40-immortalized *Bax/Bak*$^{-/-}$ MEFs. This study was supported in part by grants for Scientific Research on Priority Areas, Center of Excellence Research, the twenty-first century COE Program, and Scientific Research, from the Ministry of Education, Science, Sports and Culture of Japan, and by a grant for Research on Dementia and Fracture from the Ministry of Health, Labour and Welfare of Japan.

COMPETING FINANCIAL INTERESTS

The authors declare that they have no competing financial interests.

Received 12 July 2004; accepted 5 October 2004
Published online at http://www.nature.com/naturecellbiology.

1. Baehrecke, E. H. How death shapes life during development. *Nature Rev. Mol. Cell Biol.* **3,** 779–787 (2002).
2. Clarke, P. G. Developmental cell death: morphological diversity and multiple mechanisms. *Anat. Embryol. (Berl.)* **181,** 195–213 (1990).
3. Tsujimoto, Y. Cell death regulation by the Bcl-2 protein family in the mitochondria. *J. Cell. Physiol.* **195,** 158–167 (2003).
4. Lindsten, T. *et al.* The combined functions of proapoptotic Bcl-2 family members bak and bax are essential for normal development of multiple tissues. *Mol. Cell* **6,** 1389–1399 (2000).
5. Wei, M. C. *et al.* Proapoptotic BAX and BAK: a requisite gateway to mitochondrial dysfunction and death. *Science* **292,** 727–730 (2001).
6. Zong, W. X., Lindsten, T., Ross, A. J., MacGregor, G. R. & Thompson, C. B. BH3-only proteins that bind pro-survival Bcl-2 family members fail to induce apoptosis in the absence of Bax and Bak. *Genes Dev.* **15,** 1481–1486 (2001).
7. Bursch, W. The autophagosomal-lysosomal compartment in programmed cell death. *Cell Death Differ.* **8,** 569–581 (2001).
8. Kabeya, Y. *et al.* LC3, a mammalian homologue of yeast Apg8p, is localized in autophagosome membranes after processing. *EMBO J.* **19,** 5720–5728 (2000).
9. Mizushima, N. *et al.* Dissection of autophagosome formation using Apg5-deficient mouse embryonic stem cells. *J. Cell Biol.* **152,** 657–668 (2001).
10. Liang, X. H. *et al.* Induction of autophagy and inhibition of tumorigenesis by beclin 1. *Nature* **402,** 672–676 (1999).
11. Kihara, A., Kabeya, Y., Ohsumi, Y. & Yoshimori, T. Beclin-phosphatidylinositol 3-kinase complex functions at the trans-Golgi network. *EMBO Rep.* **2,** 330–335 (2001).
12. Liang, X. H. *et al.* Protection against fatal Sindbis virus encephalitis by beclin, a novel Bcl-2-interacting protein. *J. Virol.* **72,** 8586–8596 (1998).
13. Chen, J. *et al.* bcl-2 overexpression reduces apoptotic photoreceptor cell death in three different retinal degenerations. *Proc. Natl Acad. Sci. USA* **93,** 7042–7047 (1996).
14. Fannjiang, Y. *et al.* BAK alters neuronal excitability and can switch from anti- to pro-death function during postnatal development. *Dev. Cell* **4,** 575–585 (2003).
15. Cheng, E. H. *et al.* Conversion of Bcl-2 to a Bax-like death effector by caspases. *Science* **278,** 1966–1968 (1997).
16. Lin, B. *et al.* Conversion of Bcl-2 from protector to killer by interaction with nuclear orphan receptor Nur77/TR3. *Cell* **116,** 527–540 (2004).
17. Shimizu, S., Eguchi, Y., Kamiike, W., Matsuda, H. & Tsujimoto, Y. Bcl-2 expression prevents activation of the ICE protease cascade. *Oncogene* **12,** 2251–2257 (1996).
18. Kuma, A. *et al.* The role of autophagy during the early neonatal starvation period. *Nature* (in the press).

THE JOURNAL OF BIOLOGICAL CHEMISTRY

Vol. 279, No. 50, Issue of December 10, pp. 52726–52734, 2004
Printed in U.S.A.

Fzo1, a Protein Involved in Mitochondrial Fusion, Inhibits Apoptosis*

Received for publication, August 4, 2004, and in revised form, September 28, 2004
Published, JBC Papers in Press, September 30, 2004, DOI 10.1074/jbc.M408910200

Rie Sugioka, Shigeomi Shimizu, and Yoshihide Tsujimoto‡

From the Laboratory of Molecular Genetics, Department of Post-Genomics & Diseases, Osaka University Medical School, and Solution-Oriented Research for Science and Technology of Japan Science and Technology Corporation, 2-2 Yamadaoka, Suita, Osaka 565-0871, Japan

Mitochondrial morphology and physiology are regulated by the processes of fusion and fission. Some forms of apoptosis are reported to be associated with mitochondrial fragmentation. We showed that overexpression of Fzo1A/B (rat) proteins involved in mitochondrial fusion, or silencing of Dnm1 (rat)/Drp1 (human) (a mitochondrial fission protein), increased elongated mitochondria in healthy cells. After apoptotic stimulation, these interventions inhibited mitochondrial fragmentation and cell death, suggesting that a process involved in mitochondrial fusion/fission might play a role in the regulation of apoptosis. Consistently, silencing of Fzo1A/B or Mfn1/2 (a human homolog of Fzo1A/B) led to an increase of shorter mitochondria and enhanced apoptotic death. Overexpression of Fzo1 inhibited cytochrome *c* release and activation of Bax/Bak, as assessed from conformational changes and oligomerization. Silencing of Mfn or Drp1 caused an increase or decrease of mitochondrial sensitivity to apoptotic stimulation, respectively. These results indicate that some of the proteins involved in mitochondrial fusion/fission modulate apoptotic cell death at the mitochondrial level.

Apoptosis plays an important role in various biological events in metazoans, including development and maintenance of tissue homeostasis. A family of cysteine proteases called caspases cleaves various cellular proteins and thus drives the process of apoptosis. It has been shown that the mitochondria play a pivotal role in apoptosis by releasing several apoptogenic molecules (such as cytochrome *c*, Smac/DIABLO, Omi/HtrA2, AIF, and endonuclease G) into the cytoplasm from the intermembrane space, after which these molecules activate downstream destruction programs, including the caspase cascade (1). The pro-apoptotic increase of mitochondrial membrane permeability is mainly regulated by members of the Bcl-2 family of proteins (2–4). Bcl-2 family consists of anti-apoptotic members such as Bcl-2 as well as pro-apoptotic members, including multidomain members such as Bax and Bak and numerous BH3-only proteins (*e.g.* Bid). BH3-only proteins, when activated, transmit apoptotic signals to the mitochondria to activate Bax and Bak (which act as a gateway), leading to mitochondrial membrane permeabilization (5, 6). The apoptotic mitochondrial membrane permeabilization may also be influenced by the mitochondrial physiological status, including respiration, lipid context, and fusion/fission (7).

Mitochondria are continuously fusing and dividing, processes that are thought to have a role in homeostasis. In *Saccharomyces cerevisiae*, fission of the outer mitochondrial membrane is driven by Dnm1p, Fis1p, and Mdv1p (8–10), whereas Mdm33p is involved in fission of the inner mitochondrial membrane (11). Dnm1p is a dynamin-related GTPase that is normally localized in the cytosol (8); it undergoes translocation and binds to the outer membrane via Fis1p during fission (9) and is thought to form a large oligomeric ring-like complex that pinches the outer mitochondrial membrane. Deletion of any of the fission genes blocks mitochondrial fission and produces a fused, interconnected mitochondrial network. Orthologs of Dnm1p have been characterized in *Caenorhabditis elegans* (DRP1) (12) as well as in mammals (Drp1) (13). Fzo1p and Ugo1p drive fusion of the outer mitochondrial membrane (14–16), whereas Mgm1p is involved in fusion of the inner mitochondrial membrane (17) in *S. cerevisiae*. Fzo1 was first characterized in *Drosophila melanogaster* and is a large GTPase that circumscribes the outer membrane and is essential for mitochondrial fusion (18). Mutations of the *fzo* gene in flies inhibit mitochondrial fusion during spermatogenesis, leading to a "fuzzy onion" morphology (18). A homolog of Fzo1 protein is found in mammals (*e.g.* rat Fzo1 and human Mfn) (19, 20). Defects of yeast fzo1 or the mammalian homologs of Fzo1 result in extensive fragmentation of the mitochondria and lead to cells being classed as the ρ^0 phenotype, which lacks mitochondrial DNA (14).

Recent studies have suggested that the processes of mitochondrial fusion/fission are somehow involved in the regulation of apoptosis. During the early stage of apoptosis, the mitochondrial network is destroyed in mammalian cells (21–23). It has also been shown that overexpression of a dominant-negative Drp1 mutant (Drp1K38A) prevents apoptotic fragmentation of the mitochondrial network, as well as the occurrence of cytochrome *c* release, and apoptosis (21). Furthermore, silencing of Opa1 (a human homolog of Mgm1p) and overexpression of Fis1 both induce mitochondrial fragmentation, and reportedly also induce apoptosis (24, 25). However, the mechanisms by which fusion and fission processes are involved in apoptosis remain to be elucidated.

In the present study, we confirmed that mitochondrial fragmentation occurred during apoptosis in some cell lines. We also found that increasing or decreasing the expression of proteins involved in mitochondrial fusion (Fzo1/Mfn) relative to proteins involved in fission (Dnm1/Drp1) resulted in cells becoming more resistant or more sensitive to apoptotic stimulation, re-

* This work was supported in part by a grant for Scientific Research on Priority Areas, by a grant for Center of Excellence Research, a grant for the 21st century COE Program, by a grant for Scientific Research from the Ministry of Education, Science, Sports and Culture, and by a grant for Research on Dementia and Fracture from the Ministry of Health, Labor and Welfare of Japan. The costs of publication of this article were defrayed in part by the payment of page charges. This article must therefore be hereby marked "*advertisement*" in accordance with 18 U.S.C. Section 1734 solely to indicate this fact.

‡ To whom correspondence should be addressed. Tel.: 81-6-6879-3363; Fax: 81-6-6879-3369; E-mail: tsujimot@gene.med.osaka-u.ac.jp.

spectively, by influencing the activation of Bax/Bak in the mitochondria.

EXPERIMENTAL PROCEDURES

Chemicals and Antibodies—Bismaleimidohexane was obtained from Pierce. The caspase inhibitor z-VAD-fmk[1] was purchased from Peptide Inc. (Minoh, Japan).

An anti-Bax polyclonal antibody (N-20) and anti-Bak monoclonal antibody (Ab-1) were obtained from Santa Cruz Biotechnology (Santa Cruz, CA) and Oncogene (Boston, MA), respectively. Anti-Drp1 and anti-Tom20 monoclonal antibodies were purchased from Transduction Laboratory (San Diego, CA). Anti-human Fas monoclonal antibody (CH-11), anti-cytochrome *c* (6H2 and 7H8) monoclonal antibodies, and goat anti-mouse Alexa Fluor 488 antibody were obtained from MBL (Nagoya, Japan), BD Pharmingen, and Molecular Probes (Eugene, OR), respectively. Anti-GAPDH antibody and anti-porin (voltage-dependent anion channel) monoclonal antibody were purchased from Chemicon (Temecula, CA) and Calbiochem, respectively.

Cell Culture and DNA Transfection—HeLa cells (a human cervical carcinoma cell line) and a derivative cell line with stable overexpression of human Bcl-2 (26) were maintained in RPMI1640 medium supplemented with 10% fetal bovine serum. Rat1 cells (a rat fibroblast cell line) were grown in Dulbecco's modified Eagle's medium supplemented with 10% fetal bovine serum. SV40 T antigen-transformed wild type (WT) and Bax/Bak double knockout MEFs were grown in modified Dulbecco's modified Eagle's medium containing 10% fetal bovine serum.

To visualize mitochondria in living cells, DNA encoding Su9-DsRed2 was used: this fusion construct was produced by insertion of the presequence of mouse F_1F_0 ATPase subunit 9 into the DsRed2-N1 vector plasmid. DNA encoding truncated human Bid inserted into the pUC-CAGGS expression vector (27) and DNAs encoding rat Fzo1A/B inserted into the pCMV14 expression vector (Sigma) were also used. Cells (1×10^6) were transfected with plasmid DNA using the Amaxa electroporation system according to the supplier's protocol (kit V, program U-20). The efficiency of transfection was more than 75% as assessed by cotransfection of Su9-DsRed2 DNA. All the siRNAs used were produced by Dharmacon Research, and the sequences were as follows (numbers in parentheses indicate nucleotide positions within the respective open reading frame): rat Fzo1A-siRNA (46–66), 5′-AAGGACAAGCGACAC-AUGGCU-3′; rat Fzo1B-siRNA (110–130), 5′-AAGCAACAUACAGGA-ACCCGG-3′; rat Dnm1-siRNA (96–116), 5′-AACUCAGAGCAGUGGA-AAGAG-3′; human Mfn1-siRNA (46–66), 5′-AAGGGGAUUACUGCA-AUCUUU-3′; human Mfn2-siRNA (52–72) 5′-AAGAGACACAUGGCU-GAGGUG-3′; human Drp1-siRNA (96–116) 5′-AACGCAGAGCAGCG-GAAAGAG-3′; and GFP-siRNA (274–294), and 5′- GGCUACGUCCA-GGAGCGCACC-3′. Cells (Rat1 or HeLa cells) were transfected twice on alternate days with 10 μg of siRNA using the Amaxa electroporation system.

Analysis of Mitochondrial Morphology and Immunocytochemistry—HeLa cells, Rat1 cells, and MEFs were transiently transfected with Su9-DsRed2, and mitochondrial morphology was analyzed under a fluorescence microscope (Zeiss; LSM510META). To determine the localization of Drp1, HeLa cells were grown in 8-well chamber slides and then fixed in 4% paraformaldehyde for 20 min at room temperature, permeabilized with 0.1% Triton X-100 for 20 min at room temperature, and blocked with 2% bovine serum albumin in PBS for 30 min at room temperature. Next, the cells were incubated with anti-Drp1 monoclonal antibody for 1 h at room temperature. After washing with PBS, the cells were stained with goat anti-mouse Alexa Fluor 488 antibody, washed twice with PBS, and examined under a confocal microscope.

Subcellular Fractionation—To assess Bax translocation and cytochrome *c* release, subcellular fractionation was performed using digitonin, as described previously (28). Briefly, after washing twice with PBS, cells were suspended in buffer (20 mM potassium HEPES, pH 7.4, 10 mM KCl, 1.5 mM $MgCl_2$, 250 mM sucrose, 0.1 μM phenylmethylsulfonyl fluoride, and 1 mM dithiothreitol), and treated with 30 μg/ml digitonin for 5 min at 37 °C. Centrifugation was used to separate the cytosolic and organellar fractions, followed by lysis with radioimmune precipitation assay buffer (50 mM Tris-HCl, pH 7.5, 150 mM NaCl, 1% Nonidet P-40, 0.5% deoxycholate, and 0.1% SDS). Isolation of the heavy membrane fraction enriched in mitochondria for measurement of Drp1 was done as described previously (29). Finally, aliquots of each fraction were subjected to Western blot analysis.

Analysis of Protein Oligomerization—Oligomerization of Bak was investigated by gel filtration chromatography. HeLa cells were harvested, washed twice with PBS, and lysed with HNC buffer (25 mM sodium HEPES, pH 7.5, 300 mM NaCl, 2% CHAPS, 1 mM dithiothreitol, and 0.1 μM phenylmethylsulfonyl fluoride). After sonication and centrifugation (15,000 rpm for 15 min), the cell extract was collected and loaded onto a Superdex 200 HR 10/30 column (Amersham Biosciences) equilibrated in HNC buffer without dithiothreitol. Fractions of 96 μl were collected, and aliquots of each fraction were subjected to Western blotting.

To detect oligomerization of Bax, HeLa cells were treated with etoposide, harvested, and washed twice with PBS. Then the cells were resuspended in PBS, and Me_2SO (control) or bismaleimidohexane was added at a final concentration of 0.1 mM. After incubation for 30 min at room temperature, the cells were collected and resuspended in protein sample buffer containing dithiothreitol to quench the cross-linking reaction.

Analysis of Cell Death—HeLa cells and Rat1 cells were treated with 200 μM etoposide or 1 μg/ml anti-human Fas antibody (CH-11). Apoptotic cells were detected by examination of nuclear morphology after staining with Hoechst 33342 (1 μM).

Permeabilized Cells—HeLa cells grown in 10-well poly-L-lysine-coated glass slides, washed twice with isotonic buffer (20 mM potassium HEPES, pH 7.4, 1.5 mM $MgCl_2$, 10 mM KCl, 250 mM sucrose), permeabilized with 20 μg/ml digitonin for about 4 min at room temperature, and then washed with isotonic buffer. Permeabilized cells were incubated with recombinant human Bid protein for 10 min at 37 °C, washed with isotonic buffer, and fixed with 4% paraformaldehyde. Then the fixed cells were stained with anti-Bak (Ab-1) or anti-cytochrome *c* antibodies for 1 h at room temperature.

RESULTS

Apoptotic Mitochondrial Fragmentation and Translocation of Drp1 Are Bcl-2-independent Processes—Recent studies have shown that fragmentation of the mitochondrial network occurs during an early stage of apoptosis (21, 29, 30). To confirm this, HeLa cells were transiently transfected with DNA encoding mitochondria-targeting DsRed2 and then treated with etoposide (an inhibitor of topoisomerase II). By transfection of cells with this plasmid, the mitochondria were specifically stained red irrespective of their membrane potential (data not shown). Whereas many mitochondria were elongated and created a network in healthy cells, the mitochondria became fragmented after addition of etoposide (Fig. 1, *A* and *B*), confirming previous observations (21, 29, 30). This change occurred at an early stage of apoptosis and was not affected by the caspase(s) inhibitor z-VAD-fmk or by Bcl-2 overexpression (Fig. 1, *A* and *B*), both of which almost completely inhibited apoptosis (Fig. 1*B*), suggesting that apoptotic mitochondrial fragmentation is a Bcl-2-insensitive and caspase-independent process. Apoptotic mitochondrial fragmentation was also observed when cells were subjected to other stimuli, such as anti-Fas and staurosporine, and also when other cell lines (COS7 and Rat1) were tested (data not shown). However, mouse embryonic fibroblast cells (MEFs) showed very limited mitochondrial fragmentation during etoposide-induced apoptosis (Fig. 1*C*).

To examine whether the mitochondrial fission machinery was involved in apoptotic mitochondrial fragmentation, we examined the localization of a mitochondrial fission protein Drp1, which has been reported to accumulate in the mitochondria during fission as well as apoptosis in some cell lines (21, 30). Subcellular fractionation analysis revealed that etoposide induced translocation of a significant amount (approximately one-fifth) of Drp1 to the mitochondria (Fig. 1*D*). This was also confirmed by immunofluorescence study: after the cells were treated with etoposide, colocalization of Drp1 with Su9-DsRed2 increased as judged by significant increase of *yellow color* in the *merged photos* (Fig. 1*E*). Although etoposide-treated MEFs

[1] The abbreviations used are: z-VAD-fmk, benzyloxycarbonyl-VAD-fluoromethyl ketone; MEF, mouse embryonic fibroblast; siRNA, small interference RNA; PBS, phosphate-buffered saline; CHAPS, 3-[(3-cholamidopropyl)dimethylammonio]-1-propanesulfonic acid; GAPDH, glyceraldehyde-3-phosphate dehydrogenase.

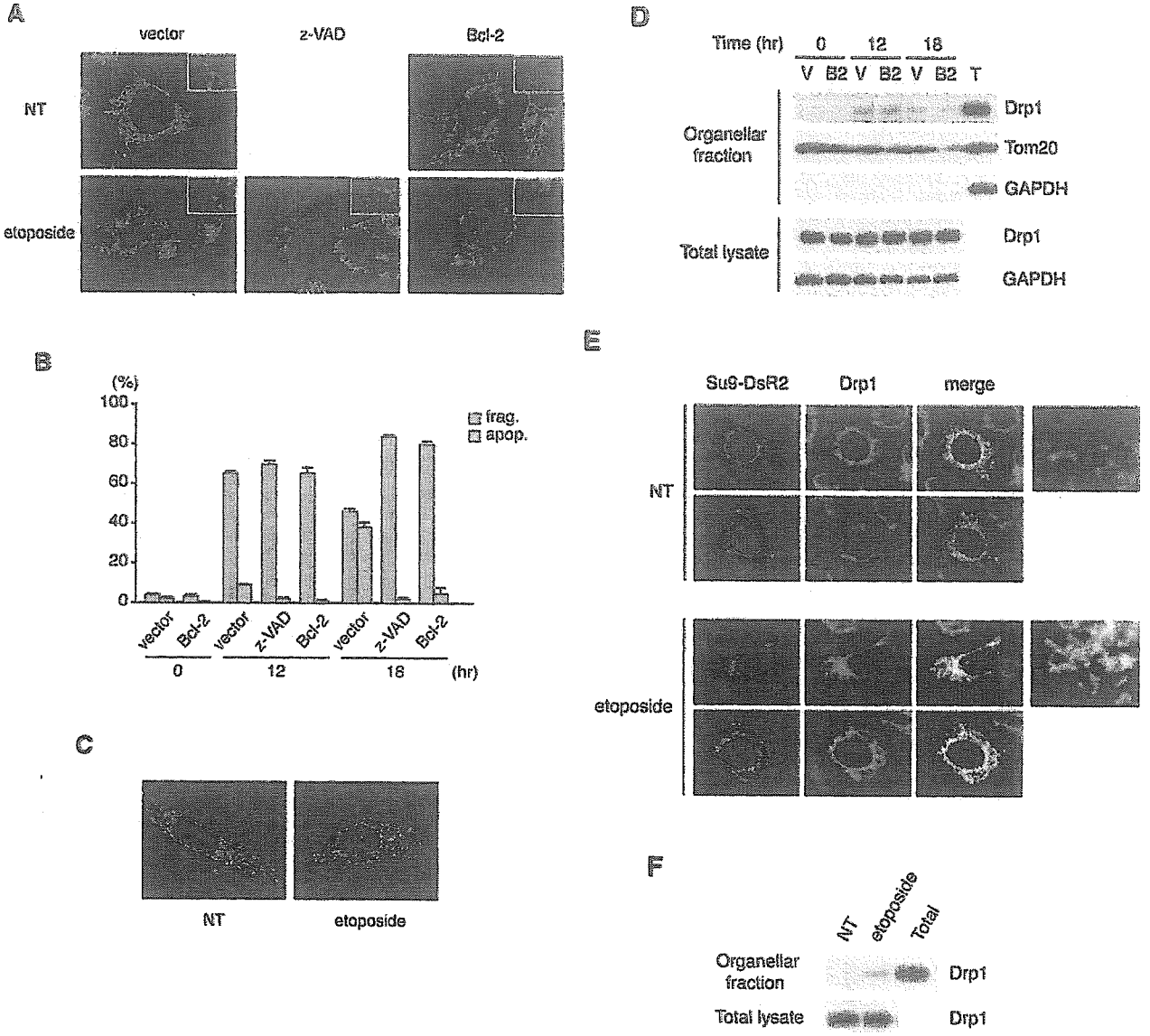

FIG. 1. **Induction of mitochondrial fragmentation and translocation of Drp1 at an early stage of apoptosis in a Bcl-2-independent manner.** *A* and *B*, no effect of Bcl-2 and z-VAD-fmk on etoposide-induced mitochondrial fragmentation. HeLa cells and HeLa cells overexpressing human Bcl-2 were transfected with DNA encoding Su9-DsRed2 (0.05 μg) and were treated with 200 μM etoposide for 16 h (*A*) or for the indicated times (*B*) in the presence or absence of z-VAD-fmk (100 μM). Mitochondrial morphology was observed under a confocal fluorescence microscope. *A*, representative images are shown. Magnified views (*frag.*) are shown in *insets*. *B*, cells with fragmented mitochondria were counted under a confocal microscope. A punctiform mitochondrial phenotype was defined as a loss of the majority of the tubular mitochondria. Apoptotic cells were counted by examination of nuclear morphology after staining with Hoechst 33342. The mean ± S.D. of three independent experiments is shown. *C*, etoposide-induced mitochondrial fragmentation in MEFs. MEFs were transfected with Su9-DsRed2 DNA (0.05 μg) and were treated with 10 μM etoposide for 16 h in the presence of z-VAD-fmk (100 μM). Then mitochondrial morphology was observed using a confocal fluorescence microscope. Representative images are shown. *D*, no effect of Bcl-2 on translocation of Drp1 during apoptosis. HeLa cells (*V*) and HeLa cells overexpressing human Bcl-2 (*B2*) were treated with etoposide. At the indicated times, the mitochondrial fraction was isolated and translocation of Drp1 was evaluated by Western blotting. Tom20 and GAPDH were monitored to verify successful fractionation and equal loading. "*T*" represents the same amount of total lysate. *E*, accumulation of Drp1 to the mitochondria after etoposide treatment. HeLa cells were transfected with DNA encoding Su9-DsRed2 and were treated with 200 μM etoposide. After 16 h, the cells were fixed and stained with anti-Drp1 (*green*) antibody. *F*, etoposide-induced translocation of Drp1 to the mitochondria in MEFs. Cells were transfected with Su9-DsRed2 DNA (0.05 μg) and treated with 10 μM etoposide for 16 h in the presence of z-VAD-fmk (100 μM). Then the mitochondrial fraction was isolated and translocation of Drp1 was evaluated by Western blotting.

showed little apoptotic mitochondrial fragmentation (Fig. 1*C*), there was significant translocation of Drp1 to the mitochondria as in HeLa cells (Fig. 1*F*). These results suggested that mitochondrial fragmentation varies between cell lines while a similar extent of Drp1 translocation to the mitochondria occurs during apoptosis, suggesting possible involvement of Drp1 and the mitochondrial fission apparatus in apoptotic events. Using this method, we also examined whether or not Bcl-2 had an influence on apoptotic translocation of Drp1. As shown in Fig. 1*D*, etoposide induced translocation of Drp1 that was not inhibited by Bcl-2, consistent with the lack of inhibition of apoptotic mitochondrial fragmentation (Fig. 1*A*), indicating that apoptotic translocation of Drp1 to the mitochondria occurs in a Bcl-2-independent manner.

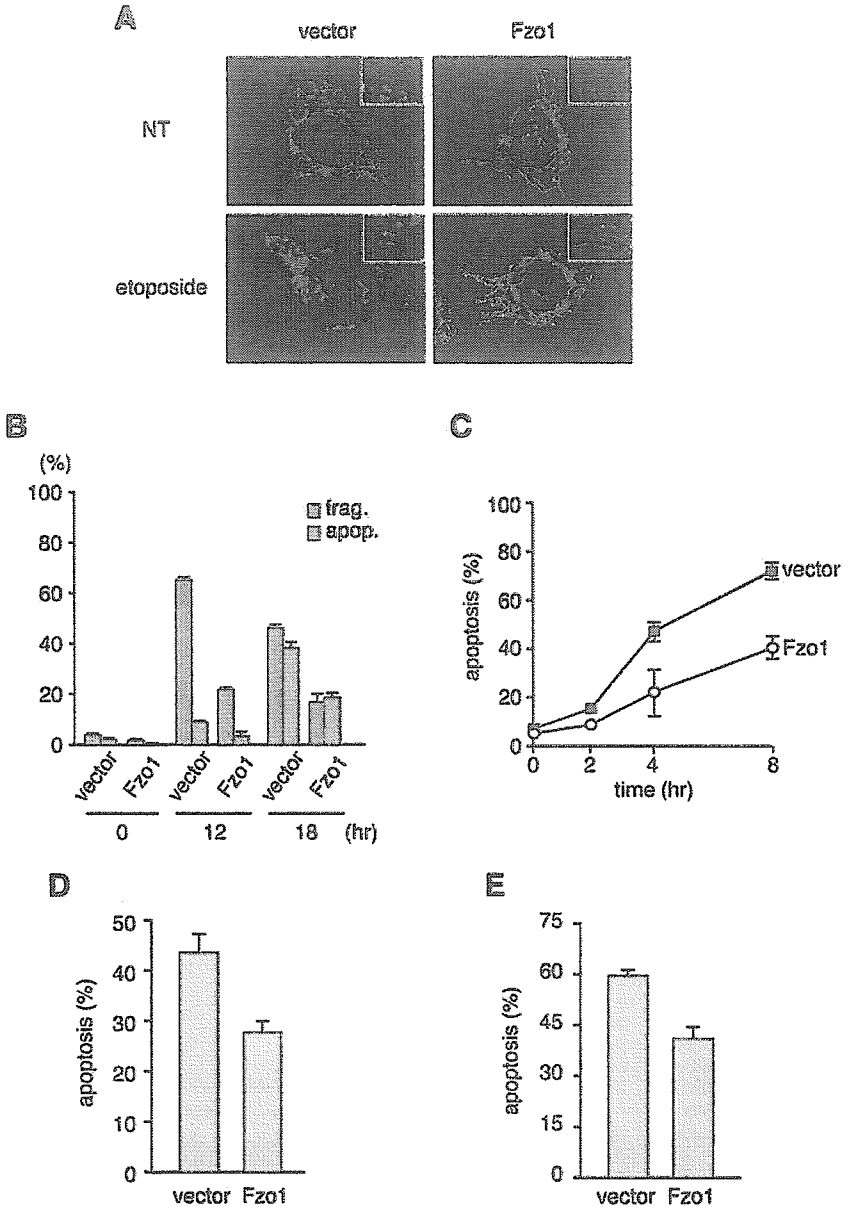

FIG. 2. **Inhibition of mitochondrial fragmentation and apoptosis by Fzo1.** *A* and *B*, inhibition of etoposide-induced mitochondrial fragmentation by Fzo1. HeLa cells were transfected with Su9-DsRed2 DNA (0.05 μg) plus 0.1 μg of empty vector or Fzo1A/B, and then were treated with 200 μM etoposide for 16 h (*A*) or for the indicated times (*B*). Mitochondrial morphology was observed using a confocal fluorescence microscope. *A*, representative images are shown. Magnified views are shown in *insets*. *B*, cells with fragmented mitochondria were counted under a confocal microscope. Then apoptotic cells were counted by examination of nuclear morphology after staining with Hoechst 33342. Data are shown as the mean ± S.D. (n = 3). *C*, inhibition of Fas-induced apoptosis by Fzo1 in HeLa cells. HeLa cells were transfected with 0.1 μg of empty vector or Fzo1A/B for 24 h and then were treated with 1 μg/ml anti-Fas antibody. At the indicated times, the cells were stained with Hoechst 33342, and apoptotic cells were counted under a fluorescent microscope. Values are the mean ± S.D. (n = 3). *D*, inhibition of etoposide-induced apoptosis by Fzo1 in Rat1 cells. Rat1 cells were transfected with 0.1 μg of empty vector or Fzo1A/B and then were treated with 200 μM etoposide. After 20 h, the cells were stained with Hoechst 33342, and apoptotic cells were counted under a fluorescent microscope. Values are the mean ± S.D. (n = 3). *E*, inhibition of etoposide-induced apoptosis by Fzo1 in MEFs. Cells were transfected with 0.3 μg of empty vector or Fzo1A/B and then were treated with 10 μM etoposide. After 16 h, the cells were stained with Hoechst 33342, and apoptotic cells were counted under a fluorescent microscope. Values are the mean ± S.D. (n = 3).

Fzo1 Inhibits Etoposide-induced Apoptotic Mitochondrial Fragmentation and Various Types of Apoptosis—We next examined whether apoptosis was influenced by the inhibition of mitochondrial fission. Rat Fzo1 (corresponding to human Mfn), an essential protein for mitochondrial fusion, was introduced into HeLa cells. Because rats have two *Fzo1* genes (*Fzo1A* and *Fzo1B*) that show 60% amino acid identity and are both essential for mitochondrial fusion (19), we introduced these two genes into HeLa cells concomitantly. Overexpression of Fzo1A/B increased elongated mitochondria (Fig. 2*A*). Not only etoposide-induced mitochondrial fragmentation, but also etoposide-induced apoptosis, was markedly delayed by Fzo1 overexpression (Fig. 2, *A* and *B*). Similar results were obtained when HeLa cells were treated with anti-Fas antibody (Fig. 2*C*), when Rat1 cells were treated with etoposide (Fig. 2*D*), and when MEFs were treated with etoposide (Fig. 2*E*). These results indicated that Fzo1A/B delays various types of apoptosis, possibly by inhibiting apoptotic mitochondrial fission.

Silencing of Fzo1 and Dnm1 (Proteins Involved in Mitochondrial Fusion and Fission) Alters Sensitivity of Cells to Apoptotic Stimuli—To determine whether alterations in the expression of genes involved in mitochondrial fusion/fission could influence the sensitivity of cells to apoptosis, we tested the effect of silencing rat Fzo1A/B and Dnm1 (a protein involved in fission) in Rat1 cells. As shown in Fig. 3*A*, Fzo1 and Dnm1 were almost completely eliminated by 48 h after the introduction of siRNA. After silencing of Fzo1, the filamentous mitochondrial network disappeared (Fig. 3*B*, *middle panel*), whereas silencing of Dnm1 resulted in the formation of elongated and interconnected mitochondria (Fig. 3*B*, *right panel*). When the cells were subsequently treated with etoposide, Fzo1-silenced cells were more sensitive to apoptosis than control cells, whereas Dnm1-silenced cells were more resistant to apoptosis (Fig. 3*C*). Similar results were obtained when HeLa cells were subjected to silencing of Mfn1/2 (the human homologs of Fzo1B/A, respectively) or Drp1 (the human homolog of Dnm1) (Fig. 3, *D* and *E*). Although cells with silencing of Fzo1A/B or Mfn1/2 showed

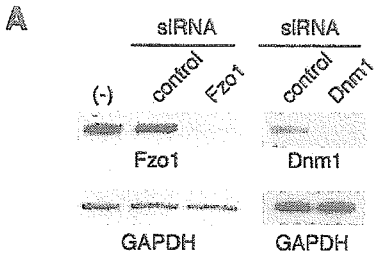

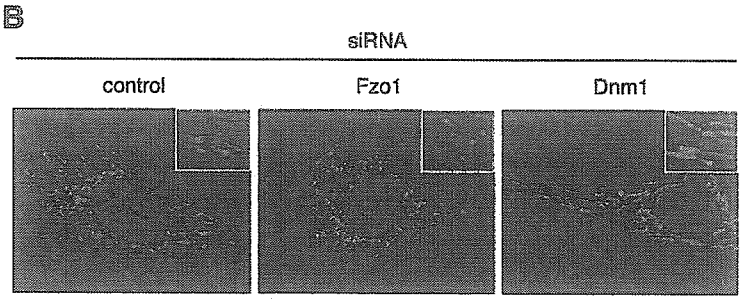

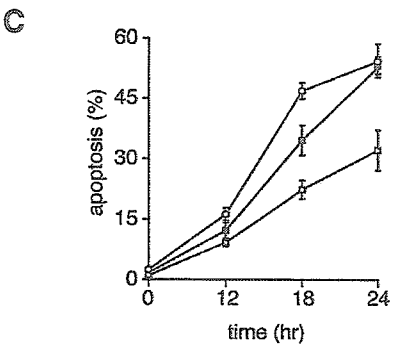

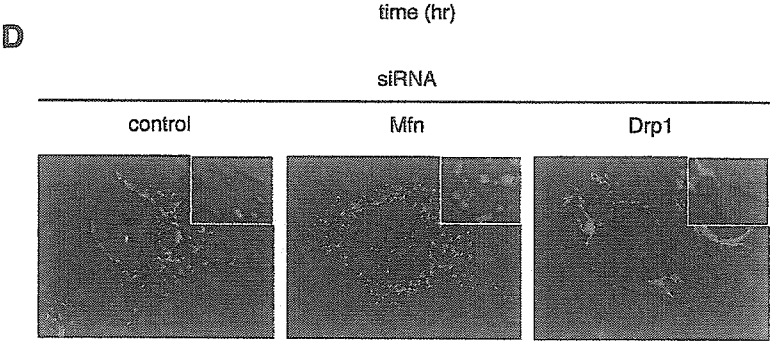

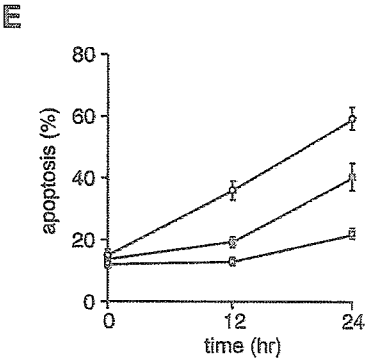

FIG. 3. **Mitochondrial fusion/fission balance affects sensitivity of cells to apoptotic stimuli.** *A–C*, the effect of silencing of Fzo1 or Dnm1 on mitochondrial morphology and apoptosis of Rat1 cells. Rat1 cells were transfected twice on alternate days with either GFP siRNA, Fzo1A/B siRNA, or Dnm1 siRNA. *A*, at 48 h after the second transfection with siRNAs, expression of Fzo1A/B, Dnm1, and GAPDH (as a control) was analyzed by Western blotting. *B*, cells were treated as in *A*, and mitochondrial morphology (detection of Su9-DsRed2) was observed using a confocal fluorescence microscope. Representative images are shown. Magnified views are shown in *insets*. *C*, at 48 h after the second transfection, cells were treated with etoposide (200 μM). At the indicated times, apoptotic cells were counted by examining nuclear morphology. *Closed squares*: GFP siRNA; *open circles*: Fzo1A/B siRNA; *open squares*: Dnm1 siRNA. Data are shown as the mean ± S.D. (n = 3). *D* and *E*, the effect of silencing Mfn1/2 or Drp1 on mitochondrial morphology and apoptosis in HeLa cells. The same experiments as in *B* and *C* were performed using HeLa cells with either GFP siRNA, Mfn1/2 siRNA, or Drp1 siRNA. *Closed squares*: GFP siRNA; *open circles*: Mfn1/2 siRNA; *open squares*: Drp1 siRNA. Data are shown as the mean ± S.D. (n = 3).

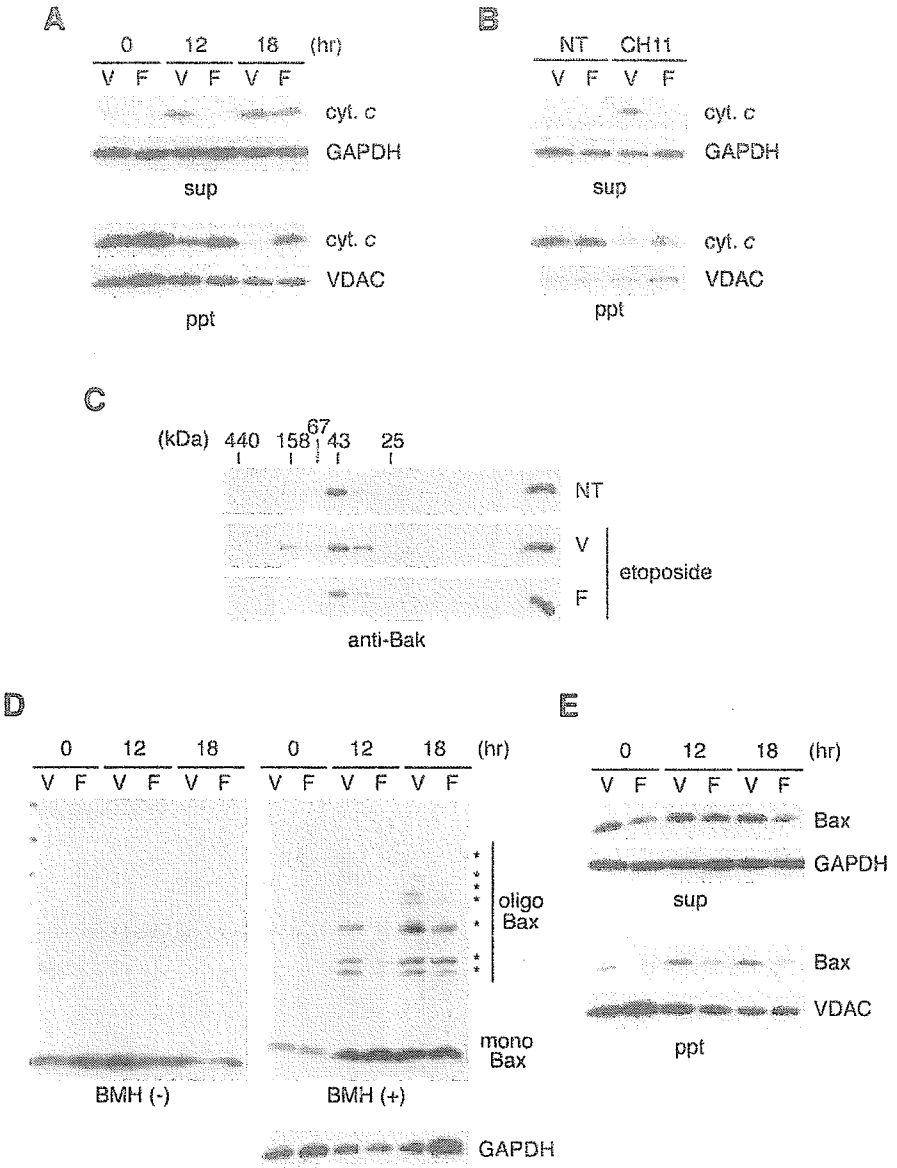

FIG. 4. **Fzo1 delays apoptosis by inhibiting Bax/Bak activation and cytochrome *c* release.** *A* and *B*, inhibition of cytochrome *c* release by Fzo1. HeLa cells were transfected with 0.1 μg of empty vector (*V*) or Fzo1A/B (*F*) and then treated with 200 μM etoposide (*A*) or 1 μg/ml anti-Fas antibody (*B*), followed by subcellular fractionation at the indicated times (*A*) or at 4 h (*B*) as described under "Experimental Procedures." The organellar (*ppt*) and cytosolic fractions (*sup*) were analyzed by Western blotting with anti-cytochrome *c*, anti-VDAC (organellar marker), and anti-GAPDH (cytosolic marker) antibodies. *C* and *D*, inhibition of etoposide-induced Bax and Bak oligomerization by Fzo1. HeLa cells were transfected with 0.1 μg of empty vector (*V*) or Fzo1A/B (*F*) and then were treated with 200 μM etoposide. *C*, after 12 h, the cells were lysed by sonication in HNC buffer and centrifuged, and the supernatants were subjected to gel filtration analysis. Aliquots of each fraction were subjected to Western blotting using anti-Bak antibody. *D*, at the indicated times, cells were incubated with Me_2SO or with 0.1 mM bismaleimidohexane. Bax oligomers (*) were detected by Western blotting using an anti-Bax (N-20) antibody. *E*, inhibition of etoposide-induced Bax translocation by Fzo1. The same experiment as shown in *A* was performed, and Bax was analyzed by Western blotting.

fragmented mitochondria, death did not occur without apoptotic stimulation (Fig. 3, *C* and *E*). All these results indicated that modulation of genes involved in mitochondrial fusion and fission could significantly influence the sensitivity of cells to apoptosis.

Fzo1 Inhibits Etoposide-induced Apoptosis by Delaying Cytochrome c Release and Bax/Bak Activation—How does Fzo1 inhibit apoptosis? Bax and Bak, which act as a gateway for various apoptotic signals at the mitochondria, are thought to exist as inactive forms in healthy cells, and various apoptotic stimuli may cause their activation through conformation changes and oligomerization, leading to cytochrome *c* release from the mitochondria (5, 6). Therefore, we first examined the effect of Fzo1 on apoptotic cytochrome *c* release in HeLa cells. As shown in Fig. 4 (*A* and *B*), Fzo1 delayed etoposide-induced and Fas-mediated release of cytochrome *c*, indicating that Fzo1 acted upstream of cytochrome *c* release. Next, we examined the effect of Fzo1 on etoposide-induced activation of Bax/Bak and found that oligomerization of both Bax and Bak was markedly delayed by Fzo1 expression (Fig. 4, *C* and *D*). Bax (but not Bak) is mainly localized in the cytoplasm of healthy cells and shows translocation to the mitochondria after apoptotic stimulation. Interestingly, overexpression of Fzo1 inhibited apoptotic mitochondrial localization of Bax (Fig. 4*E*), which might have led to

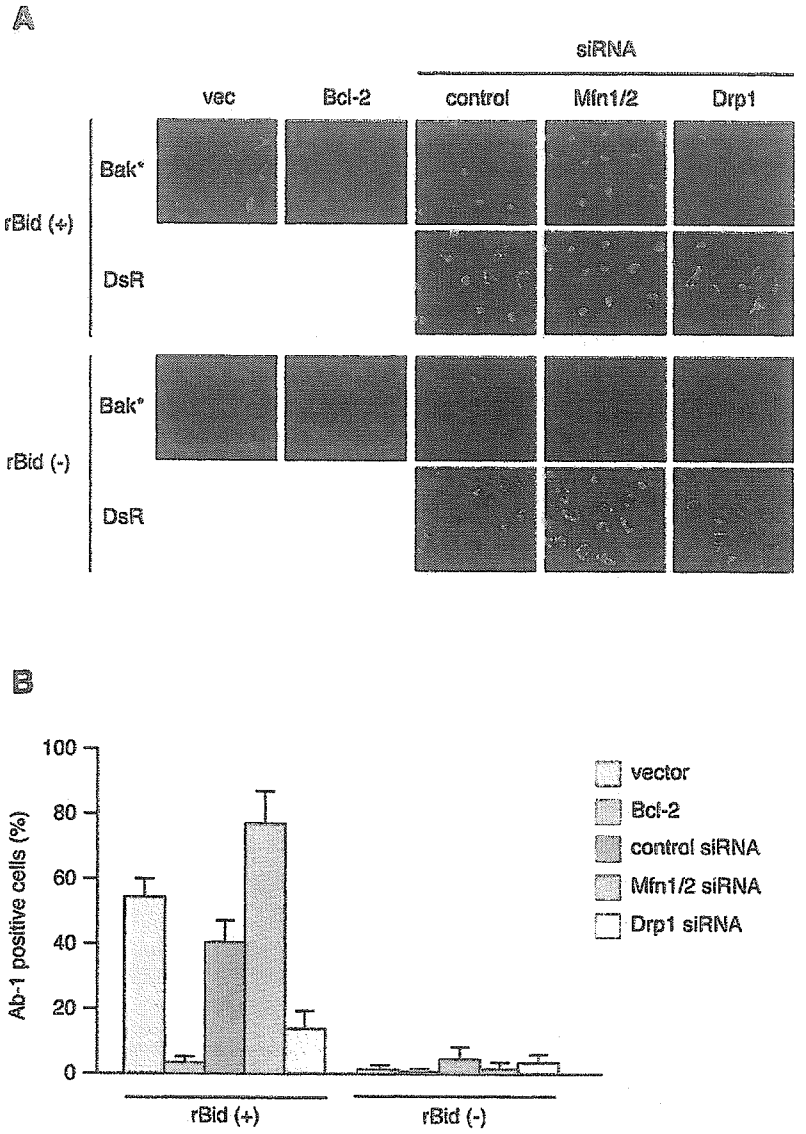

FIG. 5. **Mitochondrial fusion/fission balance affects mitochondrial sensitivity to recombinant Bid.** HeLa cells were transfected twice on alternate days with the indicated siRNAs together with Su9-DsRed2 DNA. At 48 h after the second transfection, cells were permeabilized with digitonin and then incubated with recombinant human Bid (1 μg) for 10 min at 37 °C. Next, the cells were fixed and immunostained using a conformation-specific Bak monoclonal antibody (Ab-1) that only bound to activated Bak (*A* and *B*), or an anti-cytochrome *c* monoclonal antibody (*C* and *D*). Bcl-2-overexpressing HeLa cells were used as a control. Note that cells with cytochrome *c* release did not show a cytochrome *c* signal (*arrows*) due to leakage through the permeabilized plasma membrane. *A* and *C*, representative images are shown. *B* and *D*, Ab1-positive cells (*B*) and cells with cytochrome *c* release (*D*) were counted in three randomly chosen fields under a confocal microscope. Data are shown as the mean ± S.D. (n = 3).

a delay in Bax activation. Taken together, these findings indicate that Fzo1 expression delayed the activation of Bax/Bak and thereby inhibited both cytochrome *c* release and apoptosis.

The Balance between Fusion and Fission Proteins Affects Mitochondrial Sensitivity to Death Stimuli—Changes in the levels of proteins involved in mitochondrial fusion/fission had an effect on apoptosis. Overexpression of Fzo1 inhibited apoptotic mitochondrial fragmentation and delayed Bax/Bak activation and cytochrome *c* release during apoptosis, raising the possibility that changes of the proteins involved in mitochondrial fusion/fission could alter mitochondrial sensitivity to apoptotic stimulation. To examine this issue, HeLa cells were transfected with siRNA for Mfn1/2 or Drp1, permeabilized with digitonin, and then incubated with recombinant Bid, which is a pro-apoptotic member of the Bcl-2 family and activates Bax/Bak (5, 6). Using this method, mitochondria in different states could be subjected to the same apoptotic stimulus, and the response was assessed by measuring cytochrome *c* release and Bak activation using a conformation-specific monoclonal antibody that only reacted activated Bak. Immunofluorescence microscopy demonstrated that recombinant Bid caused the activation of Bak in control cells but not in Bcl-2-overexpressing cells (Fig. 5, *A* and *B*). Because activation of Bak is cancelled by Bcl-2 in several cell lines, our *in vitro* system corresponded well with the cellular response. As shown in Fig. 5 (*A* and *B*), Mfn1/2-silenced cells largely had fragmented mitochondria and showed enhanced activation of Bak, whereas Drp1-silenced cells had elongated mitochondria and showed resistance to Bak activation. Consistent with these findings, Bid-induced cytochrome *c* release was accelerated by the silencing of Mfn1/2, whereas it was inhibited by silencing of Drp1 (Fig. 5, *C* and *D*). All these results suggested that the balance between mitochondrial fusion/fission proteins could affect mitochondrial sensitivity to apoptotic stimuli.

DISCUSSION

Here we showed that 1) mitochondrial fragmentation occurred during apoptosis and was accompanied by mitochondrial translocation of Drp1, whereas 2) changes in levels of mitochondrial fusion/fission proteins (Fzo1 (Mfn) and Dnm1 (Drp1)) affected the sensitivity of the mitochondria and cells to apoptotic stimulation. A higher fusion/fission protein ratio increased the resistance of mitochondria and cells to apoptotic stimulation, whereas a lower ratio had the opposite effect.

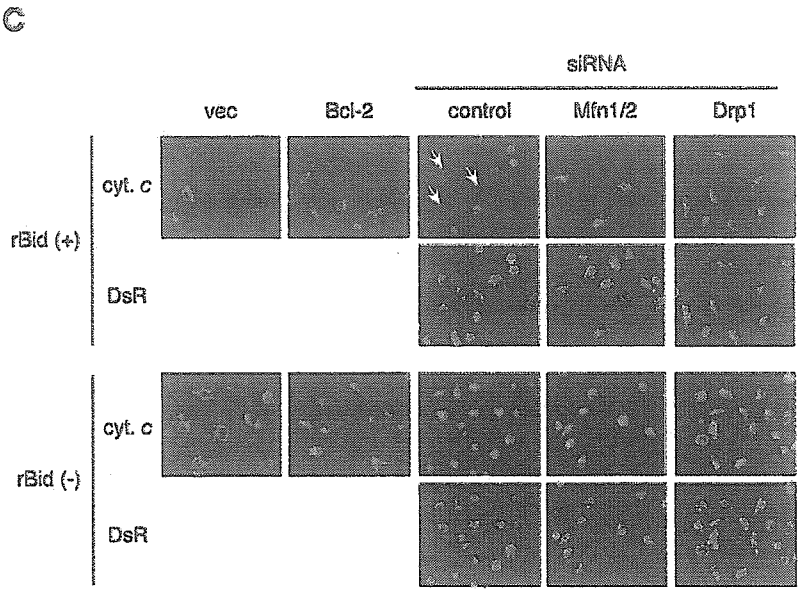

FIG. 5—*continued*

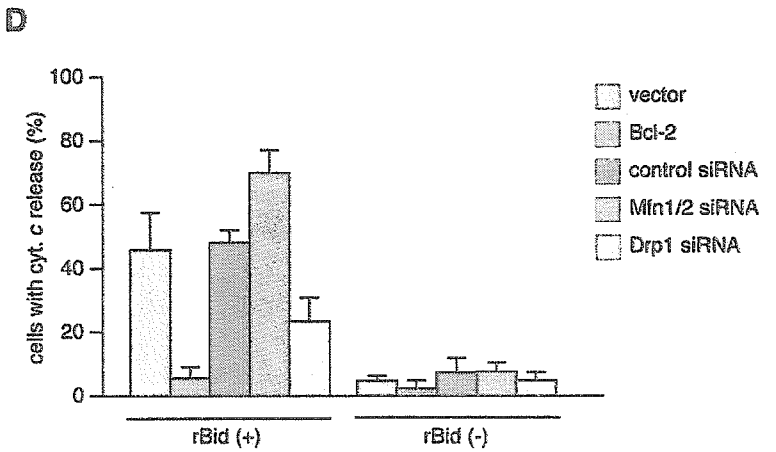

Because mitochondrial fragmentation was not observed in some cell lines, this process does not seem to be a prerequisite for apoptosis but rather to contribute to increased sensitivity to apoptotic stimuli.

How does the mitochondrial fusion/fission protein balance affect apoptosis? Although detailed mechanisms remain to be elucidated, one possibility is that, because fission and fusion of phospholipid membranes are regulated by these proteins, the mitochondrial lipid composition changes when the balance between fusion and fission protein is altered. Accumulating evidence indicates that changes of the phospholipid composition of the mitochondrial membrane can influence apoptosis. It has been reported that cardiolipin, which is a unique phospholipid in the mitochondria, is essential for the functioning of tBid during apoptosis (31) and for Bax-mediated permeabilization of liposomes (32), and that the intramitochondrial distribution of cardiolipin alters during apoptosis (33). Cardiolipin is localized in the inner mitochondrial membrane and accumulates at intermembrane contact sites (34), which have been suggested as a target for tBid and Bax (35, 36). Changes in the levels of mitochondrial fusion/fission proteins might alter the cardiolipin content of the mitochondrial membrane, thus affecting the sensitivity of the mitochondria and cells to apoptotic stimulation.

We also showed that Mfn/Fzo1-silenced cells, in which the mitochondria underwent fragmentation, did not die in the absence of additional apoptotic stimuli. These results were inconsistent with previous reports suggesting that silencing of Opa1 or overexpression of Fis1 caused both mitochondrial fragmentation and apoptosis (24, 25), so it is possible that Fis1 expression or Opa1 silencing not only provides a fission signal but also an apoptotic signal.

We also confirmed the previous observations (21, 29, 30) that Drp1 translocates from the cytosol to the mitochondria during apoptosis, although the mechanism regulating Drp1 translocation is unknown. It has been reported that a dominant negative mutant of Drp1 suppresses some forms of apoptosis (21), suggesting that the translocation of Drp1 to the mitochondria might be important for apoptosis by triggering mitochondrial fragmentation. We found that overexpression of Fzo1 significantly delayed the mitochondrial translocation of Drp1 (data not shown).

In this study, Bcl-2 did not inhibit either apoptotic mitochondrial fragmentation or translocation of Drp1 to the mitochondria (Fig. 1). We also found that apoptosis-induced transloca-

tion of Drp1 occurs equally in the absence of Bax and Bak (data not shown). Consistently, apoptotic mitochondrial fragmentation and Drp1 translocation were not observed when apoptosis was induced by overexpression of truncated Bid (tBid) (data not shown). Taken together, these results suggest that the Bcl-2 family of proteins does not seem to be involved in the processes of apoptotic mitochondrial fragmentation and Drp1 translocation, suggesting that various apoptotic stimuli (including etoposide, anti-Fas, etc.) not only activate Bax/Bak but also promote mitochondrial fragmentation that sensitizes the mitochondria to apoptotic signals.

Finally, it is interesting to note that several diseases are associated with mutations of genes involved in mitochondrial fusion/fission. Mutations of the *opa1* gene have been reported in autosomal dominant optic atrophy patients with degeneration of the retinal ganglion cells (37). Furthermore, it has been described that a mutation of the *mfn2* gene causes Charcot-Marie-Tooth neuropathy type 2A (38). It is possible that defects of mitochondrial fusion/fission might alter the susceptibility of cells to apoptotic death and, thus, cause these diseases.

Acknowledgments—We are grateful to Drs. N. Ishihara and K. Mihara (Graduate School of Medical Science, Kyushu University) for providing rat Fzo1A/B cDNAs and for helpful discussion.

REFERENCES

1. Wang, X. (2001) *Genes Dev.* **15,** 2922–2933
2. Green, D. R. (2000) *Cell* **102,** 1–4
3. Martinou, J. C., and Green, D. R. (2001) *Nat. Rev. Mol. Cell. Biol.* **2,** 63–67
4. Zamzami, N., and Kroemer, G. (2001) *Nat. Rev. Mol. Cell. Biol.* **2,** 67–71
5. Tsujimoto, Y. (2003) *J. Cell. Physiol.* **195,** 158–167
6. Danial, N. N., and Korsmeyer, S. J. (2004) *Cell* **116,** 205–219
7. Malisan, F., and Testi, R. (2003) *Curr. Med. Chem.* **10,** 1573–1580
8. Bleazard, W., McCaffery, J. M., King, E. J., Bale, S., Mozdy, A., Tieu, Q., Nunnari, J., and Shaw, J. M. (1999) *Nat. Cell Biol.* **1,** 298–304
9. Mozdy, A. D., McCaffery, J. M., and Shaw, J. M. (2000) *J. Cell Biol.* **151,** 367–380
10. Tieu, Q., and Nunnari, J. (2000) *J. Cell Biol.* **151,** 353–366
11. Messerschmitt, M., Jakobs, S., Vogel, F., Fritz, S., Dimmer, K. S., Neupert, W., and Westermann, B. (2003) *J. Cell Biol.* **160,** 553–564
12. Labrousse, A. M., Zappaterra, M. D., Rube, D. A., and van der Bliek, A. M. (1999) *Mol. Cell* **4,** 815–826
13. Smirnova, E., Shurland, D. L., Ryazantsev, S. N., and van der Bliek, A. M. (1998) *J. Cell Biol.* **143,** 351–358
14. Rapaport, D., Brunner, M., Neupert, W., and Westermann, B. (1998) *J. Biol. Chem.* **273,** 20150–20155
15. Hermann, G. J., Thatcher, J. W., Mills, J. P., Hales, K. G., Fuller, M. T., Nunnari, J., and Shaw, J. M. (1998) *J. Cell Biol.* **143,** 359–373
16. Sesaki, H., and Jensen, R. E. (2001) *J. Cell Biol.* **152,** 1123–1134
17. Wong, E. D., Wagner, J. A., Gorsich, S. W., McCaffery, J. M., Shaw, J. M., and Nunnari, J. (2000) *J. Cell Biol.* **151,** 341–352
18. Hales, K. G., and Fuller, M. T. (1997) *Cell* **90,** 121–129
19. Ishihara, N., Jofuku, A., Eura, Y., and Mihara, K. (2003) *Biochem. Biophys. Res. Commun.* **301,** 891–898
20. Santel, A., and Fuller, M. T. (2001) *J. Cell Sci.* **114,** 867–874
21. Frank, S., Gaume, B., Bergmann-Leitner, E. S., Leitner, W. W., Robert, E. G., Catez, F., Smith, C. L., and Youle, R. J. (2001) *Dev. Cell* **1,** 515–525
22. Karbowski, M., and Youle, R. J. (2003) *Cell Death Differ.* **10,** 870–880
23. Bossy-Wetzel, E., Barsoum, M. J., Godzik, A., Schwarzenbacher, R., and Lipton, S. A. (2003) *Curr. Opin. Cell Biol.* **15,** 706–716
24. Olichon, A., Baricault, L., Gas, N., Guillou, E., Valette, A., Belenguer, P., and Lenaers, G. (2003) *J. Biol. Chem.* **278,** 7743–7746
25. James, D. I., Parone, P. A., Mattenberger, Y., and Martinou, J. C. (2003) *J. Biol. Chem.* **278,** 36373–36379
26. Shimizu, S., Eguchi, Y., Kamiike, W., Matsuda, H., and Tsujimoto, Y. (1996) *Oncogene* **12,** 2251–2257
27. Niwa, H., Yamamura, K., and Miyazaki, J. (1991) *Gene (Amst.)* **108,** 193–199
28. Nomura, M., Shimizu, S., Ito, T., Narita, M., Matsuda, H., and Tsujimoto, Y. (1999) *Cancer Res.* **59,** 5542–5548
29. Breckenridge, D. G., Stojanovic, M., Marcellus, R. C., and Shore, G. C. (2003) *J. Cell Biol.* **160,** 1115–1127
30. Karbowski, M., Lee, Y. J., Gaume, B., Jeong, S. Y., Frank, S., Nechushtan, A., Santel, A., Fuller, M., Smith, C. L., and Youle, R. J. (2002) *J. Cell Biol.* **159,** 931–938
31. Lutter, M., Fang, M., Luo, X., Nishijima, M., Xie, X., and Wang, X. (2000) *Nat. Cell Biol.* **2,** 754–761
32. Kuwana, T., Mackey, M. R., Perkins, G., Ellisman, M. H., Latterich, M., Schneiter, R., Green, D. R., and Newmeyer, D. D. (2002) *Cell* **111,** 331–342
33. Garcia Fernandez, M., Troiano, L., Moretti, L., Nasi, M., Pinti, M., Salvioli, S., Dobrucki, J., and Cossarizza, A. (2002) *Cell Growth Differ.* **13,** 449–455
34. Schlame, M., Rua, D., and Greenberg, M. L. (2000) *Prog. Lipid Res.* **39,** 257–288
35. Lutter, M., Perkins, G. A., and Wang, X. (2001) *BMC Cell Biol.* **2,** 22
36. Zamzami, N., Brenner, C., Marzo, I., Susin, S. A., and Kroemer, G. (1998) *Oncogene* **16,** 2265–2282
37. Kjer, P., Jensen, O. A., and Klinken, L. (1983) *Acta Ophthalmol. (Copenh.)* **61,** 300–312
38. Zuchner, S., Mersiyanova, I. V., Muglia, M., Bissar-Tadmouri, N., Rochelle, J., Dadali, E. L., Zappia, M., Nelis, E., Patitucci, A., Senderek, J., Parman, Y., Evgrafov, O., Jonghe, P. D., Takahashi, Y., Tsuji, S., Pericak-Vance, M. A., Quattrone, A., Battologlu, E., Polyakov, A. V., Timmerman, V., Schroder, J. M., and Vance, J. M. (2004) *Nat. Genet.* **36,** 449–451